Physics – Uspekhi **50** (11) 1123 – 1146 (2007)

REVIEWS OF TOPICAL PROBLEMS PACS numbers: **97.10. – q**, 97.60.Jd, **97.80. – d**

Population synthesis in astrophysics

S B Popov, M E Prokhorov

DOI: 10.1070/PU2007v050n11ABEH006179

Contents

Abstract. Population synthesis is a method for numerical simulation of the population of objects with a complex evolution. This method is widely used in astrophysics. We consider its main applications to studying astronomical objects. Examples of modeling evolution are given for populations of close binaries and isolated neutron stars. The application of the method to studying active galactic nuclei and the integral spectral characteristics of galaxies is briefly discussed. An extensive bibliography on all the topics covered is provided.

1. Introduction

We review different aspects of astrophysical applications of the *population synthesis* method, which has become a powerful and popular research tool.

Population synthesis is the method of direct modeling of sufficiently large populations of weakly interacting individual sources with a complex intrinsic evolution. The evolution of each object is typically traced from its birth up to the current time (or one of interest). The sequence of evolutionary stages is convolved with the formation history of the objects (i.e., with their time-dependent birthrate) and the initial parameter distributions. Such a 'convolution' determines the contribution of a particular evolutionary stage of objects to the entire population. This allows studying numerous properties and observational manifestations of the studied ensemble.

In the following sections, we discuss the necessity of such modeling and provide a general description of the method (Sections 2 and 3). Then we discuss population studies of binary stars (Section 4) and isolated neutron stars (Section 5) in more detail. In Section 6, we give other examples of population synthesis studies: the calculation of integral spectra of galaxies by modeling their stellar populations and modeling the cosmic X-ray background. Some conclusions are given at the end of the review.

We only quickly touch upon many issues, and therefore references are given only to the most important papers and reviews.

Before starting the review, it seems important to make one terminological remark. There are two different methods generally referred to as *population synthesis* [1].

One method has very broad applications. In this method, the evolution of individual objects is traced from their birth with corresponding initial conditions (or from a very early time). Some authors call it the *evolutionary synthesis* (see, e.g., Ref. [1]). But a longer name is also used — *evolutionary population synthesis* (see, e.g., Refs [2 – 5]). The other method is used to study stellar populations (see Section 6.1). In [1] and some other papers, it is simply referred to as *population synthesis*. In many papers, it is called *empirical population synthesis* or *population synthesis with a database* [2]. The use of the detailed names allows separating these two methods by keeping the term 'population synthesis' in both cases.

S B Popov, M E Prokhorov Sternberg Astronomical Institute, Lomonosov Moscow State University,
Universitetskii prosp. 13, 119992 Moscow, Russian Federation
Tel. (7-495) 939 50 06. Fax (7-495) 932 88 41
E-mail: mike@sai.msu.ru, polar@sai.msu.ru

Received 17 July 2006, revised 1 June 2007
Uspekhi Fizicheskikh Nauk **177** (11) 1179 – 1206 (2007)
10.3367/UFNr.0177.200711b.1179
Translated by K A Postnov; edited by A M Semikhatov

Below, we consider only the first method (except for Section 6) and call it the *population synthesis* (PS). Hopefully, this does not lead to confusion.

2. Why population synthesis is needed in astrophysics

The necessity of PS in astrophysics is mainly due to the scientific peculiarity of astronomy. In astronomy, we cannot conduct a direct experiment with the object under investigation: the role of experiments in astronomy is played by observations. Virtually any observation of an astronomical object is a momentary 'snapshot' of the object with a very long evolutionary timescale. It is impossible to observe the evolution of an individual star or a galaxy. The evolutionary sequences of the vast majority of objects can be recovered only by modeling.

Another feature of astronomy is that "we are looking for where there is light." Most objects seen in the sky (both by the naked eye and with the use of any instrument) are not typical but rather peculiar representatives of some population (peculiar from the point of view of the terrestrial observer). In other words, "astronomy is the science about selection effects" (A V Tutukov). One may try to construct a theory describing only that small part of the particular objects being observed. But the 'correct' theory must be consistent with the existence of other objects that we do not see. Hence, the necessity emerges of studying not only individual easily observable representatives but populations of objects.

It is important to note that it is impossible to observe individual objects in many cases, because we obtain only integral characteristics of their populations (unresolved stars in remote galaxies provide an example). In this case, direct modeling of the population seems to be the most appropriate to better understand its properties.

Another feature of astronomy we need to mention is related to the very high cost of large-scale astronomical instruments (satellites, telescope networks, etc.) Their design should be adjusted to particular tasks at the early stages of their construction. In particular, when constructing a new, more powerful instrument, it would be important to know what kinds of sources, which had not been observed earlier, could be discovered. This can be achieved (partially, of course) only by analyzing available data about all known sources that can be potentially detected in the corresponding wavebands.

Two main goals of PS studies can be emphasized. The first is the testing or the determination of some parameters of the studied population of objects (for example, the initial spin period of neutron stars or their initial mass function) by comparing the actually observed and theoretically modeled populations of the sources. We are unable to directly obtain the initial parameters of objects or the parameters of their evolution in a *model-independent way*. PS is one of the available tools that allows obtaining knowledge on the unknown properties of astronomical objects by means of their modeling. Finding parameters that well describe observations would allow a quantitative explanation of the origin and evolution of the studied objects.

The ultimate application of PS allows calculating an artificial universe in detail. Should the artificial universe have the same properties as the real one, this would indicate the construction of the full self-consistent physical picture of the world that fits all theories and experiments.

Therefore, the first application of PS is in *testing the parameters and providing an explanation* of astronomical manifestations of different types of objects.

The second goal of PS is to predict properties of sources that have so far been unobserved (for example, an evaluation of the merging rate of supermassive binary black holes to be registered by the space gravitational wave detector LISA, or of the coalescence rate of binary neutron stars to be observed by the ground-based gravitational wave observatory LIGO). We note that in this case, the prediction uncertainty is mainly due to the uncertainty of the model parameters [6]. Of course, a subsequent comparison of the PS predictions with new observations is to test the assumptions made and may require changing them. Therefore, both goals are interconnected.

We now consider some basic properties of PS that can be applied to different modelings.

3. General properties of models used in population synthesis

The PS method used in astrophysics has no direct analogs in other natural sciences. For example, most objects in physics (elementary particles, atoms, molecules, etc.) are much simpler than astronomical objects and correspondingly have much simpler evolutions. On the other hand, the behavior of living organisms is much more complicated, and the interaction between individuals and different species must be taken into account.

We comment on the definition of population synthesis given in the Introduction. We stress that all parts of the definition are equally important.

(1) The considered population cannot be too small, otherwise statistical fluctuations dominate in the results of calculations. If calculations are conducted for a large number of objects, the comparison with a small actual population gives little information. A similar problem can also emerge in the case of a large population if only a few rare objects dominate in some range of the integral system parameters. For example, a few (or even one) high-luminosity stars can determine the integral color of a cluster (see papers [7–9], which discuss some restrictions of the PS application).

(2) The evolution of an individual object should not be too simple or, in contrast, too complicated. In the first case, a detailed numerical PS is not necessary at all, because analytic or semianalytic methods can be used (we note that analytic calculations were used in the early PS studies of single and binary stars in the framework of very simple models). If the evolutionary track is too complicated, it is very difficult to describe it by a numerical code; in addition, the number of different states can become too large, i.e., can much exceed the number of objects in the studied real population.

(3) Objects should not significantly interact with each other; otherwise it is impossible to construct an individual evolutionary track and the evolution of the entire population should be calculated. But interactions between objects are not absolutely forbidden in PS. For example, stars in globular clusters may interact with each other by forming and destroying binary systems. We note that here we mean the weakness or rarity of the interactions; the close fly-bys or collisions of single stars and/or binary systems we consider below provide an example. When an object is considered as a whole, internal interactions can be arbitrarily strong as, for example, the interaction between the components of a close binary system.

From the 'philosophical' standpoint, PS calculations can be divided into two stages:

• the calculation of the model population;

• the calculation of values (or distributions) based on the model population.

The quantities of interest can include: the number of sources of a certain type or with certain parameters, the mean or extreme values of the object parameters or the statistical moments of these parameters, correlation coefficients between pairs of parameters, and parameter distributions (one- or multidimensional, in the differential or cumulative form).

If the population of sources is not the aim of the modeling by itself, it can be constructed implicitly. In this case, the problem of the parameter calculations (or their distributions) reduces to calculating some multidimensional integrals of a complex function expressed via the evolutionary scenario of the objects. To calculate these integrals, regular multidimensional grids or the Monte Carlo method can be used. Each method has its own advantages and drawbacks.

In PS modeling, the integration method (the classical grid or Monte Carlo) determines the way of setting the initial parameters of individual objects. The chosen range of the initial parameters must cover the entire region of the initial conditions of the model system. This covering must be sufficiently homogeneous. If the integrals are calculated by the classical means, the chosen region is covered by a (quasi) rectangular grid, not necessarily homogeneous. In the Monte Carlo method, the initial conditions are chosen randomly with statistical weights proportional to their realization probability.

If the model sample of an object is to be compared with observations, only the second method (Monte Carlo) can be used, because the sample parameters obtained by regular methods keep the information on the grid that was used in choosing the initial parameter values.

3.1 Errors in the population synthesis method and their sources

Sources of errors in PS calculations deserve separate consideration. The various reasons for the errors include:

• insufficient accuracy of models;

• a sparse network of high-accuracy models and the need for their interpolation;

• incomplete account of physical processes;

• numerical errors and random errors;

• normalization.

We consider these errors in more detail. As noted above, the calculation of a sufficiently large model population of studied objects (at present, hundreds of thousands or millions of individual objects) is an important step of population modeling. The initial parameters of individual objects from such a population are chosen randomly (in the Monte Carlo method) or in a regular way in the studied region. In both cases, evolutionary tracks should be constructed for a large number of objects with different initial parameters.

The evolutionary model included in the PS code allows direct calculations. But detailed calculations of the evolution of astronomical objects are frequently very tedious. In this case, specially calculated grids of evolutionary tracks that include the desired parameter ranges are used in PS. Evolutionary tracks for intermediate values of parameters can be obtained by interpolating over the grid parameters. Such an approach is widespread but has two related problems.

First, due to the complexity of the detailed evolutionary calculations, the basic grid of tracks is quite sparse, and the parameters of the neighboring calculations differ by not less than 1.5–2 times. As a result, the evolution of neighboring objects on the basic grid can be quite different, which causes problems with the interpolation of evolutionary tracks to the intermediate values of the initial parameters.

Second, the sparse grid of evolutionary tracks can miss important evolutionary channels.

Typical examples of these approaches are as follows. The magnetorotational evolution of neutron stars can be described by a simple analytic model based on the angular momentum balance [10]. Despite its simplicity, this model quite well corresponds to the present understanding of the physics of spin-up and spin-down of magnetized neutron stars. This model can be incorporated into the evolutionary code, which allows direct calculations of the individual evolutionary tracks for each object from the model population.

A simple empirical description of the common envelope evolution may provide another, even clearer example. At this stage, one of the stars of a very close binary system (usually a compact object) penetrates the dense outer layers of the nondegenerate companion, which leads to the effective ejection of the shell and rapid spiral-in of the binary components. The hydrodynamic modeling of this stage is a very complicated physical and numerical problem. Such calculations are quite rare (see review [11]) and the obtained results are widely different. To describe this stage empirically, two very simple models based on the exchange of energy [12, 13] or the angular momentum [14] have been proposed (see Section 4.3 for more details). These formulas can be directly included into any PS code but yield strongly different predictions: according to the energy formula, the binary components are found to approach much closer.

Typical examples of interpolation include the calculation of the thermonuclear evolution of stars (from the main sequence to the end of the thermonuclear evolution and the formation of compact objects) and of the thermal evolution (cooling) of young hot neutron stars. At present, grids of evolutionary tracks of normal stars and grids of cooling neutron stars are available. But in both cases, the values of the main parameters of the neighboring tracks are different by dozens of per cent, or even by several times or orders of magnitude for the secondary parameters.

There are examples of the potential missing of evolutionary stages under an insignificant (by a fraction of a per cent) variation in the stellar mass. Such stages are missed on the grid with a mass step of dozens of per cent.

The interpolation of the parameters of evolutionary tracks with widely different initial conditions is a separate issue. We consider how this is done for evolutionary tracks of normal stars. In these tracks, one marks the typical points (for example, the zero-age main sequence, leaving the main sequence, the complete exhaustion of hydrogen in the center, helium ignition, the appearance of layer burning). The interpolation (with respect to the time and the initial parameters) is performed between these points. Usually, the power-law interpolation (linear for logarithmic values of the parameter and time) is used. This is justified by the following arguments: main-sequence stars with close masses have a similar structure, with their evolutionary times being power-

law functions of time. After the main sequence, this similarity disappears and the power-law interpolation becomes a source of additional errors in the modeling.

Additional errors can also be due to numerical methods used in the PS. Numerical errors of general methods (such as interpolation, integration, finding roots of equations, numerical solution of differential equations, etc.) are well known; the Monte Carlo method brings some random errors into the results. But there are also errors specific to PS calculations.

The appearance of such an error can be illustrated by the following example. Any dependence of the star formation rate on time can be described as a sequence of populations of equal-age objects (the number of objects in these populations can be very different). This approach requires the knowledge of the evolutionary isochrones for stars of different ages. The isochrones include evolutionary parameters for the population of equal-age objects with different initial properties (for example, masses for normal stars). Sometimes, isochrones are calculated together with evolutionary tracks, but in most cases are obtained by interpolating evolutionary tracks, and therefore the transition from a track to an isochrone introduces additional errors specific to the PS method.

The incompleteness of the physical model is a separate topic. For example, the present accuracy of stellar nuclear evolution calculations (without rotation and magnetic fields) is better than 1%. However, this accuracy is excessive, because a typical stellar population contains at least 10% of close binaries with much less certain evolutions and parameters than are known for single stars of the same mass. This addition significantly reduces the accuracy of stellar population parameters.

Finally, the normalization of the results of calculations should be mentioned. For the comparison with observations, the model results should be appropriately normalized (to increase the statistical accuracy in the Monte Carlo modeling, one usually calculates many more objects than are actually observed). The normalization coefficients are known to within a factor of 2, as a rule. The fraction of binaries among the total stellar population, the fraction of radio pulsars among young neutron stars, etc. may provide an example. Absolute normalization can be done using normalization by the galactic rate of supernova explosions, by the total mass of the modeled stellar cluster, etc. The comparison of calculations with observations for well-modeled systems sometimes allows increasing the accuracy of the normalizing coefficients by using the PS method itself.

Some aspects of PS uncertainties are considered in more detail in [9].

4. Population synthesis of close binary systems

In this section, we consider the PS of binary stars focusing on close massive binaries. The evolution of the components of a close binary system differs significantly from the evolution of single stars; the nuclear evolution of a massive star occurs on a short time scale and results in the appearance of compact objects: neutron stars, white dwarfs, and black holes.

4.1 Evolution of stars

Here, we give an introduction to the PS of binary stars and provide brief information that is necessary to understand the results discussed below. The detailed description of the physics of processes occurring in massive stars and compact objects, as well as their formation, can be found in well-known monographs, which have already become textbooks (see, e.g., [15, 16] and the references therein). A complete, although somewhat obsolete description of the evolutionary scenario, including the evolution of compact objects, can be found in [10],[1] and its updated version in [17]. Later publications [18–20] are added to different parts of this review. A very detailed description of the evolution of close binaries with compact companions is given in Ref. [21].

4.1.1 Formation of stars. Stars are formed as a result of the collapse and subsequent fragmentation of giant molecular clouds. Protostars are formed from the densest fragments. Then they gradually contract and pass through different evolutionary stages (a very short adiabatic contraction, then isothermal contraction, the Hayashi stage, where the star is fully convective and its material is strongly mixing, and the pre-main sequence star stage — objects like FU Ori, T Tau, etc.), and finally become main-sequence stars. Usually, most of the molecular cloud is dispersed during the collapse, and hence the formed stars turn out to be gravitationally unbound and escape their birthplace. Such expanding groups of young stars are called stellar associations. We note that the whole group of stars produced from one cloud is gravitationally unbound. But individual stars in this group can form gravitationally bound systems: binary stars (most frequently), hierarchical multiple binary systems, and open clusters.

The process of star formation from the interstellar medium is as interesting and complicated as stellar evolution. A detailed review can be found in [22, 23]; a more popular description is given in [24].

We note that except for protostellar evolutionary studies, all PS calculations start from the main sequence. Information on the protostellar evolution is then substituted by the distribution of stellar parameters in the zero-age main sequence. (In some cases, for example, in studies of neutron stars and radio pulsars, the consideration starts from even later stages, after the formation of a compact object.)

4.1.2 Single stars. We start with a very brief description of the evolution of single stars. Thermonuclear reactions provide the source of energy in normal stars. The normal star spends most of its time[2] in the main sequence, when hydrogen is burning into helium in its center. All the energy is released in the stellar core that comprises about 10% of the mass within a very small fraction of the stellar radius. The energy released in the center is carried towards the surface by convection and/or radiation transfer, and is emitted from the surface with a spectrum similar to the black-body one. The main stellar parameters — luminosity, surface temperature, and nuclear time scale — are mainly determined by the stellar mass. The higher the mass of the star, the higher its luminosity and temperature are and the shorter its thermonuclear evolution is.

After some time, hydrogen in the stellar core is fully exhausted. This signals the end of the main-sequence stage.[3]

[1] See the electronic version of this review at http://xray.sai.msu.ru/~mystery/articles/review/.

[2] About 90% of its lifetime, but it somewhat depends on the mass of the star.

[3] This statement applies only to stars with a mass in excess of $0.8M_{\odot}$ ($M_{\odot}$ is the solar mass, which is about 2×10^{33} g). Less massive stars spend time in the main sequence exceeding the age of the Universe; their post-main-sequence evolution is interesting only theoretically.

A helium core is formed in the star. Because there are no sources of energy in the core, it becomes isothermal, loses gravitational energy, and contracts. During the contraction, the temperature in the core increases such that hydrogen starts burning in the adjacent thin layer (so-called hydrogen shell burning). The rate of energy release significantly increases, leading to convection in the stellar envelope. The envelope strongly expands and its surface temperature decreases. The star becomes a bright red giant or supergiant. In the Hertzsprung – Russell diagram (the color – luminosity of the color – absolute stellar magnitude diagram), the star moves off the main sequence towards the red-giant branch.

During the formation and expansion of the convective envelope, the core continues contracting and heats up. After some time, the temperature reaches $\sim 10^8$ K and the density is 10^4 g cm^{-3}, with the result that thermonuclear burning of helium begins — the so-called triple alpha-process, whereby three ^{4}He nuclei (α-particles) form one ^{12}C nucleus (in stars with masses below $0.5M_\odot$, this never occurs: helium cannot burn inside such stars). The stellar parameters during the helium core burning somewhat differ from those during the hydrogen shell burning, and the star moves from the red-giant branch to the horizontal branch in the Hertzsprung – Russell diagram.

When all the helium in the core is burned out to produce carbon, the carbon core starts contracting and heats up, and the helium shell source appears near the core, while hydrogen shell burning continues in the upper layers. A deep convective zone is formed above the shell burning sources, which mixes the rest of the envelope from the shell burning sources up to the surface. After helium shell burning has started, the star moves to the asymptotic-giant branch in the Hertzsprung – Russell diagram.

After some time, the temperature and density in the carbon core increase such that thermonuclear burning of carbon and oxygen starts. In the cores of the most massive stars, the thermonuclear burning of heavier elements proceeds up to the formation of iron-peak elements (Fe, Ni, Co). The core of the star gradually acquires a more and more complicated 'onion-like' structure.

As new central and shell burning sources switch on, the size and luminosity of the star change such that it moves in a complex way in the Hertzsprung – Russell diagram (Fig. 1).

The most massive stars have a very strong stellar wind, which strengthens at later evolutionary stages. In some cases, the matter outflow is so large that the star entirely loses its hydrogen envelope and the naked helium core remains. These objects are called Wolf – Rayet (WR) stars.[4]

The end product of the thermonuclear evolution of a star depends on its mass. In stars with masses $\lesssim 8M_\odot$, a degenerate carbon – oxygen core (possibly involving other elements lighter than iron) is formed. At the final stages, the envelope of the star is dispersed by forming a planetary nebula and the core cools to form a white dwarf.

In more massive stars, the core remains nondegenerate until the formation of the iron-peak elements. Thermonuclear synthesis stops at the iron-peak elements because thermonuclear reactions occurring after that consume energy. The iron core of a star loses its stability and collapses. This process is accompanied by a huge gravitational energy release. The envelope is rapidly ejected and expands, and its luminosity increases for some time — we observe the explosion of a core-collapse supernova (of type II, Ib, or Ic). The central parts of the collapsing core form a neutron star or a black hole in the most massive stars.[5] We refer the reader to review [26] for a more detailed description of the late evolutionary stages of massive stars.

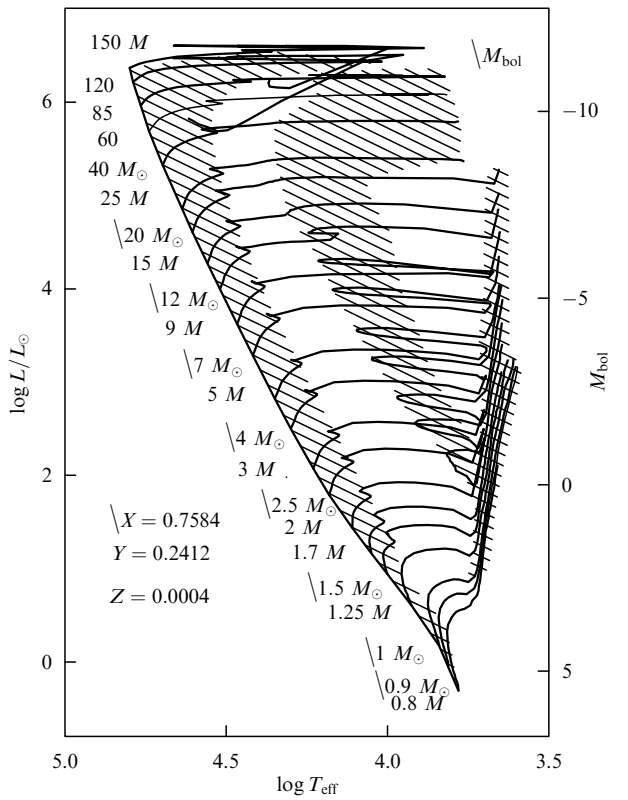

Figure 1. Evolutionary tracks of single stars with masses from 0.8 to 150 $M_\odot$. The slowest evolution is in the hatched regions [25].

The further fate of a compact object is different. In binary systems, black holes can increase their mass. Their angular momentum can also be increased by the accretion of matter. At the same time, isolated black holes can be regarded as virtually nonevolving objects.

The principal evolution of a white dwarf is its cooling. In a binary system, a white dwarf can increase in mass to reach the Chandrasekhar limit, after which the white dwarf collapses and a type-Ia supernova explodes. For white dwarfs, the magneto-rotational evolution can also be significant.

Neutron stars in binary systems demonstrate the most diverse astrophysical appearances. Thermal radiation from the neutron star surface can be observed. Neutron stars can accrete matter with a huge energy release, and can be observed as radio pulsars or via the interaction of their magnetic field with the surrounding plasma. The main

[4] Another way of forming a WR star is via hydrogen envelope loss during mass exchange in a close binary system. Much less massive WR (helium) stars can be formed in binaries. WR stars also have a very strong stellar wind, such that some of them can lose the helium envelope until the appearance of the naked carbon or nitrogen core — the so-called Wolf – Rayet stars of class WC or WN, respectively.

[5] In fact, the process is more complicated: only the most massive stars can form black holes; however, under some conditions, neutron stars can also be formed from them. The exact value of the initial mass of a star capable of producing a black hole is poorly known. Its lower bound is estimated to be $25M_\odot$ (see, however, Ref. [43]). All these processes are described in detail in [26].

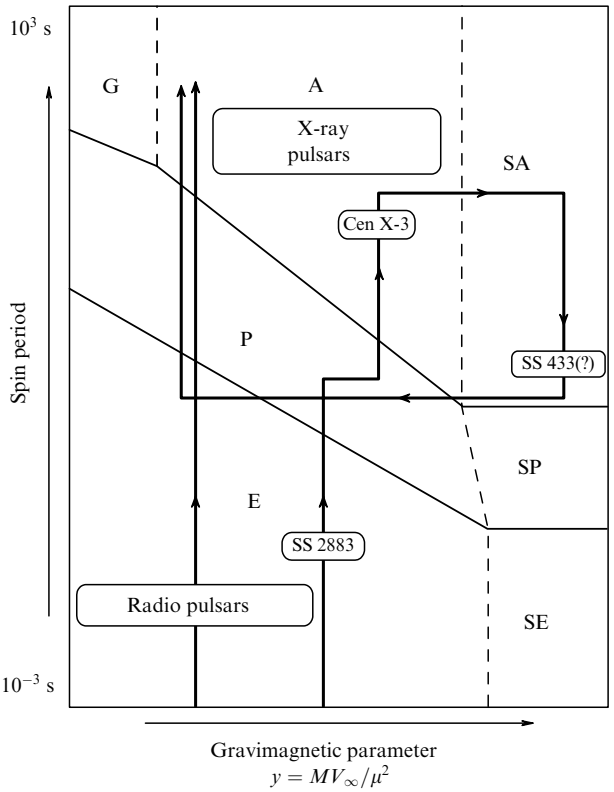

Figure 2. The spin evolution of neutron stars with nondecaying magnetic fields [10]. The left track corresponds to a single radio pulsar: the rotation period increases, the neutron star magnetic field and interstellar parameters are virtually constant. The track therefore looks like a segment of a straight line. The second track corresponds to the evolution of a neutron star in a binary system. The spin period first increases during the initial ejection stage, then stops increasing at the accretion stage and the subsequent superaccretion stage, where the neutron star spins up. After the end of thermonuclear evolution of the secondary component, the neutron star starts evolving similarly to a single radio pulsar in the interstellar medium.

parameters that determine the astrophysical manifestations of a neutron star include its surface temperature, the spin period, and the surface magnetic field (together with the physical parameters of the ambient medium). It is possible to differentiate between two quite independent types of evolution of neutron stars — thermal evolution and magneto-rotational evolution. In some neutron stars these processes occur almost independently, but in other neutron stars (for example, in magnetars), they are tightly connected. There are several possible paths the neutron star spin period evolution can take (neglecting the possible decay of the neutron star magnetic field) (Fig. 2).

The core collapse leading to the formation of neutron stars occurs asymmetrically. As a result, the young neutron star can acquire a sufficiently high spatial velocity (up to several hundred km per second), the so-called kick velocity. These velocities are inferred from radio pulsar proper motion measurements. Black holes can also be formed with a kick if their formation occurs through an intermediate stage with a hot neutron star.

The evolution of compact objects is described in more detail in Section 5.

4.1.3 Binary stars. The thermonuclear evolution of stars in binary systems mainly proceeds in a way similar to the

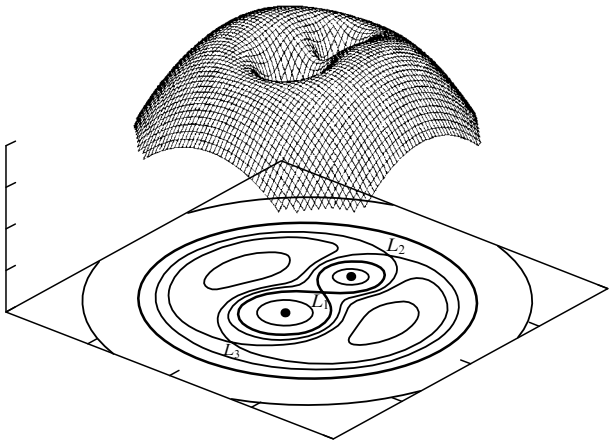

Figure 3. Three-dimensional representation of the gravitational potential of a binary star (in a corotating frame) and several cross sections of the equipotential surfaces by the orbital plane. The Roche lobe is shown by the thick line [27].

evolution of single stars. The presence of the secondary component leads to the following differences:

(1) the effect of the secondary-component stellar wind;

(2) tidal effects and tidal synchronization of the rotation of the components;

(3) the mass transfer and accretion of matter.

We note that the first two effects only weakly influence the evolution of binary stars. The effects of stellar wind collisions and interaction with the surrounding interstellar medium can be easily observed, especially around massive luminous stars, but are virtually unimportant for the structure and physical processes in close binaries. Tidal effects are more important. For example, the accuracy of theoretical evolutionary models of single stars allows measuring the rotational period change due to the tidal synchronization.

Mass transfer is the most significant effect. A single nonrotating star has a spherical form (all equipotential surfaces of a spherically symmetric gravitational potential are spheres). In a binary system, this is no longer the case. However, the asphericity is small as long as the size of the star is much less than the distance between the components. As the size of stars in a binary system increases, their surfaces deviate more and more from the spherical shape and, at some critical size, merge to form one equipotential surface comprising both components. The critical surface is similar to two pear-like bodies touching at their tips (Fig. 3). Each figure is called a Roche lobe. The singular point of this surface is called the Lagrangian point L_1. At this point, the gravitational potential of the system (in the corotating reference frame) has a saddle-point singularity and the gravitational potential gradient (i.e., the gravity acceleration) vanishes. [6]

If the size of a star exceeds its Roche lobe (this is possible when the radius of the star increases during the evolution, for example, off the main sequence, or when the orbital major semiaxis decreases), the matter in the vicinity of the inner

[6] There are five Lagrangian points at which the gravitational attraction force is compensated by the centrifugal force. Here, the orbit of the system is assumed to be circular and stars are point-like masses. The potential is written in the frame corotating with the orbital revolution. All five points lie in the orbital plane. Three of them lie in the line connecting the centers of the stars. The other two form right triangles with the binary components.

Lagrangian point starts flowing to the second component. The flow represents a narrow stream that ends either on the surface of the second component or in the accretion disc around it. The former situation is possible when the second component is also a nondegenerate star and has a sufficiently large radius. If the second component is a compact star, an accretion disc is usually formed around it.

Several solar masses of matter can be transferred from one star to another during the mass exchange in a binary system. The mass exchange results in several interesting possibilities. For example, the mass of a main-sequence companion can increase and its subsequent nuclear evolution is then significantly accelerated; the hydrogen envelope of a red giant (supergiant) can be totally lost and the naked helium core can appear; the mass of the compact star (a white dwarf or a neutron star) can exceed the upper limit and the star can then collapse, etc. Accretion of matter is accompanied by angular momentum transfer, resulting in a significant spin-up of the secondary component: a normal star becomes a Be-star, white dwarfs spin-up to second periods, and neutron stars become millisecond pulsars. In addition, accretion onto compact stars is accompanied by a powerful energy release in UV or X-ray bands (for white dwarfs and neutron stars, respectively).

During the Roche-lobe overflow, the mass exchange between the binary components can be so intensive that the secondary component is unable to accommodate all of the accreting matter. This can happen if the accretor is a nondegenerate star whose mass is much smaller than the primary-component mass or during a strongly super-Eddington accretion onto a compact object. [7]

4.2 History of the PS of binary systems

The first population studies of binary stars were carried out at the end of the 1980s (see, e.g., Refs [28, 29]) The authors of these papers used evolutionary scenarios elaborated by Paczynski, Kippenhahn, Weigert, Iben, and many others (see reviews [30, 31]).

The next stage in binary PS studies started after the appearance of sufficiently complete realizations of evolutionary scenarios. Below, we list some actively working groups that elaborated their own codes. For these groups, PS is one of the principal fields. The list is presented in chronological order (the order of the PS code design), and gives references to the published description of the PS code and the results that are most interesting in our opinion.

• V M Lipunov et al.: a detailed description of the 'Scenario Machine' and a review of first results is given in [10]. Other studies: The rate of cosmological supernovae [32], binary black-hole merging rates [33], and the increase in the masses of neutron stars and black holes [34, 35]. The description of the last version of the 'Scenario Machine' is given in [17].

• L R Yungelson et al.: binary white dwarfs and type-Ia supernovae [36 – 38], stellar sources of gravitational waves [39], etc.

• J Hurley, O Pols et al.: 'blue strugglers' [40], tidal effects in binary systems [41].

• S E Portegies Zwart, F Verbunt et al.: PS of dense stellar clusters [44], black holes of intermediate masses [45, 46], etc. Their code (for massive binaries) is partially described in [47].

• P Podsiadlowski et al.: the evolution of compact binaries and neutron star kicks [48 – 50], hypernovae and gamma-ray bursts [51], etc. The evolutionary scenario used by this group is described in [52].

• V Kalogera et al.: binary neutron star coalescences and their gravitational wave emission [53, 54], radio pulsars, neutron stars and black holes [55, 56]. A detailed description of the new version of the PS code (StarTrack) is given in Refs [57, 58].

• B Willems et al. [59]: BiSEPS (Binary Stellar Evolution and Population Synthesis). The main subjects of their studies include binary white dwarfs and millisecond pulsars [61].

We note that initially these groups worked independently, but currently many of them conduct joint research [42]. We also note that the use of a PS code based on an incomplete evolutionary scenario to specific studies has currently become common practice.

4.3 Census of compact stars and their distributions

The PS of binary systems is a very useful tool for statistical studies of binaries with compact objects. Typical examples of problems to be investigated by PS include:

• How many different compact objects are formed?

• What is their mass distribution?

• What is the relation between the original masses of stars and masses of compact objects formed in binaries?

• What would be the relative fractions of different compact objects (e.g., neutron or quark stars and black holes) for the given critical masses?

• What are the evolutionary stages, in which order are they realized, and how many binaries can be found at these stages?

Figure 4 taken from [20] illustrates such studies.

In what follows, we describe some results that partially answer these questions. Before discussing the results of binary PS studies, we make two remarks. First, these results are based on using different evolutionary tracks of normal stars (in the form of analytic approximations, stellar evolutionary track libraries, etc.), different initial parameter distributions (the initial binary mass ratio, neutron star kicks, magnetic fields, etc.), and very different assumptions on complex evolutionary stages (such as the common envelope, the accretion induced collapse, mergings, etc.). Second, in spite of some diversity in the results of calculations, they are very similar and stable in general.

4.4 Cataclysmic variables

Cataclysmic variables are binary stars that consist of an accreting white dwarf and a small-mass main-sequence star filling its Roche lobe. Permanent contact with the Roche lobe is sustained by the orbital angular momentum removal via magnetic stellar wind or gravitational wave emission. The magnetic stellar wind is related to convective motions in the envelope of the normal star. The mechanism is effective for

[7] The Eddington luminosity $L_{\rm Ed}$ is the luminosity of a massive object when the radiation pressure is balanced by the attraction of the central mass. (Because both the radiation pressure and the gravitational attraction change proportionally to $1/r^2$, their ratio is distance-independent.) The radiation pressure depends on the state of the matter and the radiation spectrum. Usually, the accreting material is the fully ionized plasma in which Thomson scattering is the dominant mechanism of interaction with radiation. In that case,

$$L_{\rm Ed} = \frac{4\pi G M m_{\rm p} c}{\sigma_{\rm T}} \approx (1.3 \times 10^{38}\ {\rm erg\ s^{-1}})\ \frac{M}{M_\odot}\,,$$

where M is the mass of the object, G is the gravitational constant, $m_{\rm p}$ is the proton mass, c is the speed of light, and $\sigma_{\rm T}$ is the Thomson scattering cross section.

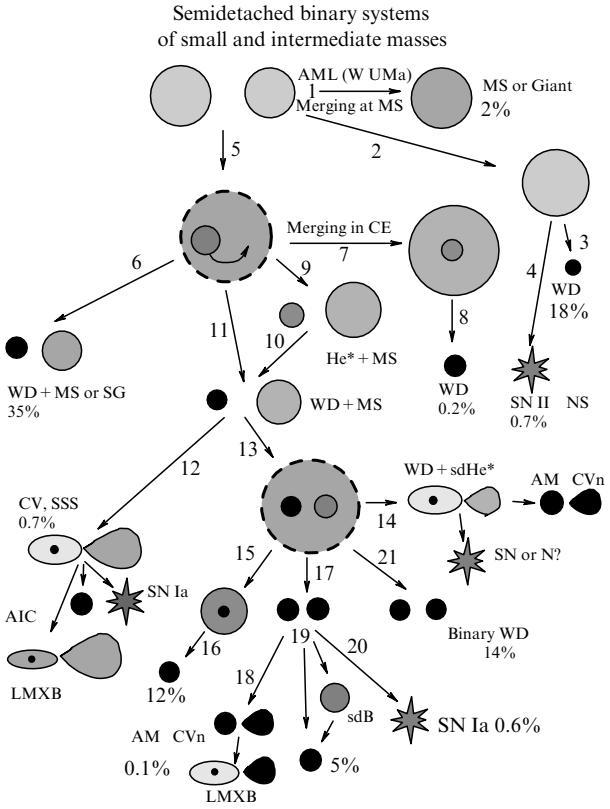

Figure 4. A small part of the evolutionary scenario of close binary systems [20]. Because we do not describe single stars in detail here, the main purpose of this figure is to show the complexity of the possible evolution of binary stars. MS is the main sequence stage, the longest evolutionary stage where thermonuclear burning of hydrogen in the stellar core occurs; SG is the supergiant stage; CE is the common-envelope stage (it appears when one star enters the outer shells the other component and results in a very rapid shrinkage of the binary orbit and an intensive dispersion of the common envelope); He is a helium star, the naked nondegenerate helium core of the evolved star; N is a nova explosion; SN is a supernova explosion (SN II for type-II supernovae; SN Ia for type-Ia supernovae); AIC is the accretion-induced collapse of a white dwarf; WD is a white dwarf; NS is a neutron star; LMXB is a low-mass X-ray binary system; CV is a cataclysmic variable star; SSS is a super-soft (X-ray) source; W UMa, AM CVn are evolutionary stages named in analogy with the known prototypes of variable stars.

stellar masses $0.3-1.5\,M_\odot$. When the mass of the donor star becomes less than $\sim 0.3\,M_\odot$, the magnetic stellar wind disappears and the accretion temporarily stops. The later evolution of the system is determined by gravitational wave emission. After some time, the star again fills its Roche lobe and an X-ray source reappears.

Magnetic stellar wind causes a more powerful accretion in the system than gravitational wave emission. A brighter X-ray source therefore appears at the magnetic stellar wind stage.

This model predicts a gap in the orbital distribution of cataclysmic variables. It is actually observed near orbital periods $P_{\rm orb} \sim 3$ h. In systems with larger orbital periods, the accretion is caused by the magnetic stellar winds; in closer systems, it is due to the gravitational wave emission.

In addition to the described processes, the angular momentum loss can be due to interaction with a circumbinary disk. However, this mechanism is usually less efficient.

PS studies of cataclysmic variables (in particular, their orbital period distribution) in the framework of the standard evolutionary model have been carried out by many authors (see, e.g., Refs [66 – 68]). They have managed to reproduce the observed distribution. A PS study of cataclysmic variables surrounded by circumbinary disks was performed in [69, 70], with the conclusion that in order to explain the observed bimodal period distribution in the circumbinary disk model, a proper bimodality of various properties of such disks is required.

4.5 Binary white dwarfs

In our opinion, there are two most interesting results obtained in PS studies of binary white dwarfs.

The first is related to the so-called common-envelope (CE) stage. This stage can occur in the course of an intensive mass transfer between the components when one of them overfills its Roche lobe. If the secondary star is incapable of accommodating all the accreting matter, an outflow from its surface begins and the so-called common envelope forms around the binary system. Two- and three-dimensional hydrodynamic calculations have shown that the dispersion of the accreting matter in space is accompanied by the effective loss of orbital angular momentum. This results in a very strong and rapid shrinkage of the orbital major semiaxis. Sometimes, the common envelope stage ends with the coalescence of the binary components.

Detailed hydrodynamic calculations of this stage are very complicated and are not numerous, and the results obtained are quite different. Several analytic descriptions of this stage have been proposed. The first approach uses energy conservation. This was proposed in [12] and is now used in the form of the formula (first appearing in [13])

$$\alpha_{\rm CE}\left(\frac{GM_{\rm don}^{\rm f}M_{\rm ac}}{2A_{\rm f}}-\frac{GM_{\rm don}^{\rm i}M_{\rm ac}}{2A_{\rm i}}\right)=\frac{GM_{\rm don}^{\rm i}M_{\rm don,\,env}}{\lambda R_{\rm don,\,rl}}\,,$$

where $M_{\rm don}$ and $M_{\rm ac}$ are the masses of the donor and the accretor, $M_{\rm don,\,env}$ is the mass of the donor's envelope, $R_{\rm don,\,rl}$ is the Roche lobe radius of the donor, λ is a parameter depending on the central density concentration of the donor (of the order of unity), $\alpha_{\rm CE}$ is the common envelope efficiency, and the superscripts i and f correspond to the initial and final values of the parameters.

The second approach, which was proposed in [14] and used in [71, 72], is based on the angular-momentum conservation:

$$\frac{\delta J}{J}=\gamma\,\frac{\Delta M}{M_{\rm tot}}\,,$$

where ΔM is the mass of the common envelope, $M_{\rm tot}$ is the mass of the binary system before the start of the CE stage, and γ is the common envelope efficiency (γ can take values from 1 to 4). This approach predicts a somewhat different evolution during this stage.

Evaluating the CE efficiency has been one of the most important issues. The closest binary white dwarfs have been proposed as one of the best indicators. The number of such systems puts stringent constraints on the angular momentum lost during this stage.

Binary white dwarfs with ultra-short orbital periods result from two successive CE stages. The first CE stage is due to the primary, more massive, component's Roche lobe overflowing. The second CE stage starts when the secondary component fills its Roche lobe. According to [73, 74], the

CE efficiency is $\alpha_{CE} \simeq 0.3-0.5$. (In [74], alternative dependences were also checked.)

These studies (as well as some others) were performed under the assumption that the value of the parameter α_{CE} is the same for all systems. This estimate is inconsistent with the PS studies of binary systems, in which only one common envelope stage occurred. This condition was relaxed in papers by Politano (see, e.g., Ref. [75]). In later papers by this author [76], it is pointed out that the absence of cataclysmic variables with secondary brown dwarfs bounds the common envelope efficiency as $\alpha_{CE} < 0.1$. The last paper by this author [77] seems to be very interesting; he investigates how the dependence of the common envelope efficiency (according to the energy formula) on the mass of the secondary component affects the results of the binary-star PS calculations.

The second important issue is the study of close binary white dwarf mergings. This process is one of the evolutionary channels leading to type-Ia supernova explosions. This problem was studied in many papers [78, 53, 36]. The binary white dwarf mergings were shown to be able to explain thermonuclear supernova explosions occurring with the rate $\sim 10^{-3}$ y^{-1} in a Milky Way-like galaxy. This result holds for both young and old stellar populations, i.e., can be applicable in both spiral and elliptical galaxies.

The second formation channel of thermonuclear supernovae (the accretion onto a white dwarf in a close binary system) also significantly contributes to the total supernova rate: $\sim 10^{-4}$ y^{-1}. This channel is much more effective for young stellar populations. Modern observations show that the type-Ia supernova rate per unit mass is much higher for young stellar populations [79]. This can be used as an argument against the coalescence scenario. In addition to PS calculations, the absence of hydrogen in spectra of type-Ia supernovae is another argument against semidetached binary type-Ia progenitors.

4.6 Accreting X-ray sources and millisecond pulsars

Modern X-ray observatories like Chandra and XMM-Newton are sensitive enough to detect all bright and most of the moderate X-ray sources in the Galaxy.[8] There are many types of persistent and transient binary X-ray sources: X-ray pulsars, X-ray bursters, 'atoll' and Z-sources of quasi-periodic oscillations, X-ray novae, black hole candidates, etc. Some sources can display several of these properties. The observational properties of different types of galactic X-ray sources are reviewed in [80–82].

The first PS calculations of the evolution of massive X-ray binaries were carried out about 25 years ago [28]. PS studies of binary stars with secondary components of small and intermediate masses, which have a more complicated evolution, were done somewhat later. Recently, different authors have begun taking the individual properties of the studied regions or objects into account, for example, the history of star formation in a particular galaxy, or the mass spectrum and metallicity of a given star-forming region. Presently, these studies are very intensive, and we therefore give only a short list of publications devoted to the PS of binary X-ray sources carried out in recent years.

For example, in Ref. [84], the authors tried to reproduce about 140 actually observed small-mass X-ray binaries in our Galaxy using the standard evolutionary scenario of small- and intermediate-mass binary stars. Some inconsistencies between the model and observations were overcome in a later paper by the same authors [85], where a more detailed scenario was used. They also considered properties of millisecond pulsars.

In a series of papers by Raguzova [86], Be–X-ray sources were studied. It was assumed that the Be-star is the secondary, originally less massive, component of a large-mass close binary system. Its peculiar properties (in particular, the rapid rotation and powerful stellar wind) are explained by the accretion spin-up during the first mass transfer from the primary component. Because neutron stars in such binaries frequently have eccentric orbits, they demonstrate some interesting phenomena. Calculations showed that 70–80% of all Be-stars should have compact components.

Some studies were specially carried out before the launch of X-ray observatories. Populations of objects that can be potentially observed by a given satellite were modeled. For example, different kinds of X-ray sources observed by the Chandra observatory were studied: binary X-ray sources in the nearby star-forming galaxy NGC 5253 [87], and weak X-ray sources in the Galaxy center [88, 89].

In addition, we note two types of especially interesting (in our opinion) sources. Binary X-ray sources are different not only in the physical sense but also in the PS context. Both a numerous population of short-lived objects and a scarce population of long-lived objects can yield an equal number of observed sources. The PS of such systems is much more difficult. We briefly discuss two groups of rarely formed but long-lived sources.

The first group includes small-mass accreting progenitors of millisecond radio pulsars. The PS of millisecond pulsars and their progenitors is discussed in Refs [85, 90, 91]. The following conclusions are obtained in these papers: The number of bright sources ($L_X > 10^{36}$ erg s^{-1}) very strongly depends on the common envelope parameters; the accretion at a near-Eddington rate leads to the formation of neutron stars with masses $\sim 2-4\,M_\odot$; there are different formation channels for wide binary millisecond pulsars, one of which leads to the formation of binary systems with orbital periods ~ 10 days, while others lead to systems with orbital periods 100–200 days.

The second example of long-lived sources with a low birthrate is given by X-ray novae — close binaries consisting of an accreting black hole and a small-mass main-sequence star. To obtain such a system in the standard binary evolutionary scenario, the original binary components should have had very different masses. The black-hole progenitor should be at least as massive as $25-30\,M_\odot$. Of course, such a massive star can lose a significant fraction of its mass before the formation of a compact object. During that time interval, the small-mass component barely changes. The observed number of sources of this type was found to be difficult to reproduce by the described scenario. In 1986, Eggleton and Verbunt [92] proposed X-ray nova formation in a hierarchical triple massive binary system. The evolutionary scenario for hierarchical triple and multiple systems leads to a

[8] For example, the Chandra observatory can detect a source with the X-ray luminosity $\sim 10^{30}$ erg s^{-1} from the galactic center distance. This luminosity corresponds to the expected accretion rate onto an isolated low-velocity neutron star in the interstellar medium; in binaries, the accretion rate is usually several orders of magnitude higher. However, in the soft X-ray band where these observatories operate, interstellar absorption can be fairly strong. For example, there are galactic X-ray sources that can be observed only in hard X-rays (by telescopes of the INTEGRAL observatory).

richer variety of observational manifestations than the binary evolution scenario (see, e.g., Ref. [93]). The numerical simulation of the evolution of a triple system is very complicated. We are aware of only one example of such a code [94]. The authors of [94] compared PS simulations of X-ray novae for the binary and triple scenarios. The formation rate of X-ray novae in the triple scenario turns out to be higher and is close to the actually observed value.

It should be noted that several solutions to this problem have recently been proposed without using the evolutionary scenario of triple stellar systems, whose rate of occurrence is poorly known. Paper [95] shows that the observed rate of X-ray novae can be recovered by using the modern description of Wolf – Rayet stellar winds in PS. Paper [96] argues that the same result can be obtained by assuming a less efficient angular momentum loss in the stellar wind than in the standard scenario.

4.7 Ultra-luminous X-ray sources

Ultra-luminous X-ray sources (ULXs) are point-like X-ray sources with a very high luminosity, located outside the nucleus of host galaxies (see their catalog in [97] and [98] for a recent review). Usually, these objects are determined as sources with the X-ray luminosity exceeding $\sim 10^{39}$ erg s^{-1} (from $\sim 10^{39}$ to $\sim 10^{42}$ erg s^{-1}). The first ultra-luminous sources were discovered by the Einstein X-ray observatory [99]. A large number of such sources were discovered by the ROSAT and Chandra observatories (however, part of them may be background sources). Ultra-luminous X-ray sources are not known in our Galaxy.

There are two popular models of ULXs. In the first model, the accretion proceeds onto a black hole with the intermediate mass $10^2 - 10^3\ M_\odot$ at a rate close to the Eddington value [100] (see Ref. [101] for a detailed discussion of the properties of intermediate-mass black holes). The obvious advantage of this hypothesis is a natural explanation of the high luminosity. The main shortcoming is that intermediate-mass black holes themselves remain sufficiently hypothetical objects. Modeling of the observed source population has not yielded satisfactory results so far.

According to the other hypothesis, ULXs contain ordinary stellar-mass black holes whose radiation is collimated in narrow jet outflows. In this model, the observed flux strongly depends on the angle between the jet axis and the line of sight. If one looks along the jet, a very bright source is observed. In this model, ULXs can form the brightest tail of the black-hole luminosity distribution [102, 103].

It is quite possible that the population of ULXs consists of two (or maybe more) types of objects with different physical natures [104]. But there are no statistically significant proofs of this hypothesis.

Podsiadlowski et al. [105] systematically studied the formation and evolution of black holes in close binary systems in the framework of the 'standard' model, in which the mass of one of the binary components must be sufficiently high to allow the formation of a black hole, and the mass of the secondary component may fall within a broad interval. The components spiral in inside the common envelope. Different selection effects were taken into account in [105]. The authors concluded that this model is consistent with the observed luminosity function of these sources, including ultra-luminous ones. The evaluated number of sources per galaxy is about 0.01, which allows explaining their absence in the Milky Way.

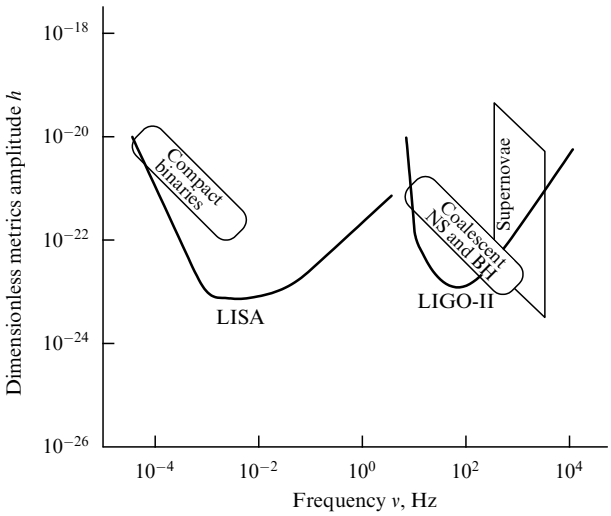

Figure 5. The sensitivity of the ground-based (LIGO-II) and space (LISA) gravitational-wave interferometers and signals from some astrophysical sources [106]. LIGO-II is the advanced LIGO interferometer with an order-of-magnitude higher sensitivity.

4.8 Contribution of binaries to the gravitational-wave background

The new generation of ground-based gravitational-wave interferometers (three detectors: LIGO, VIRGO, and GEO) and space antennas (the LISA project) is aimed at searching for gravitational waves in the respective frequency intervals $10^1 - 10^3$ and $10^{-4} - 10^{-1}$ Hz. The initial LIGO interferometer (LIGO-I) was expected to be in operation in around 2000. Astrophysical and cosmological sources of gravitational waves for this detector are reviewed in [106 – 108]. In fact, this detector started performing scientific runs in 2004; the interferometer is expected to be modified in the next few years. In this connection, much work has been done to revise earlier predictions. These results and references, as well as the first gravitational-wave data analysis, can be found in a series of papers [109].

There are three types of astrophysical sources of gravitational waves in the frequency range of the ground-based detectors[9] (Fig. 5):

(1) core collapse supernovae (of type II, Ib, or Ic);

(2) rapidly rotating axially nonsymmetric neutron stars;

(3) close binaries and coalescing compact binaries.

Estimates of the contributions of the first two types of sources to the background are not very precise. The galactic rate of supernovae is known fairly well ($\sim 1/30 - 1/50$ y^{-1}), but the uncertainty of their gravitational-wave luminosity is very large. Unfortunately, no complete theory of core collapse supernovae is known presently.

Rapidly rotating neutron stars emit monochromatic gravitational waves. Most energy is radiated at the double spin frequency (at the second harmonic). The contribution from other harmonics (the first, the third, and higher) is usually very small and depends on the detailed geometry of a neutron star. The radiation flux from such objects depends on the spin frequency and the degree of their nonsphericity. Very rapidly rotating neutron stars become axially nonsymmetric due to the Chandrasekhar – Fried-

[9] Here, we do not discuss the coalescing supermassive binary black holes that will possibly be primary sources of gravitational waves for LISA.

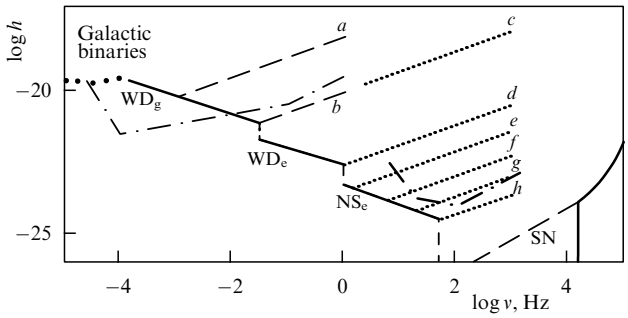

Figure 6. The gravitational-wave spectrum from close and coalescent binaries [116]. To the left: the gravitational-wave signal from binaries: points below the frequency 10^{-4} Hz show the signal from galactic main-sequence binaries, solid lines show the continuous spectrum from merging compact binaries (WD_g are galactic binary white dwarfs, WD_e are binary white dwarfs in other galaxies, NS_e are binary neutron stars and black holes in other galaxies). The dashed and dotted lines in the center show: *a* and *b*; coalescing binary white dwarfs; *c*, a merging binary neutron star in the Galaxy; *d*–*h*, merging binary neutron stars in other galaxies. To the right: the total signal from supernova explosions. All spectra are shown for a broad-band detector ($\Delta\nu \sim \nu$). The dashed-dotted line shows the sensitivity limits of LIGO-I and LISA detectors. (The figure shows the projected LIGO-I sensitivity; the actual sensitivity of no working detector can be find on the LIGO project site [117]).

man–Schutz instability [110, 111], or due to the *r*-mode instability [112, 113].

Very young neutron stars (with ages of several years) or neutron stars in accreting binary systems observed as the fastest millisecond X-ray pulsars can rotate rapidly enough to become axially nonsymmetric. In the case of accreting neutron stars, the gravitational-wave luminosity L_{GW} is well defined because it is directly related to the accretion rate and X-ray luminosity of the system (gravitational waves carry away all the angular momentum brought by the accreting matter):

$$L_{GW} \simeq L_X \,.$$

Deviations from the axial symmetry (and hence the flux of gravitational waves) depend on the viscosity and temperature in the crust and the core of the neutron star. These parameters (especially viscosity) are poorly known, with different studies giving controversial results.

The gravitational radiation from a binary star is the exact and unavoidable result of general relativity (see, e.g., Ref. [114]). The energy flux from a binary star is given by

$$L_{GW} = \frac{32}{5}\frac{G^4}{c^5}\frac{M_1^2 M_2^2 (M_1 + M_2)}{a^5} \,,$$

where M_1 and M_2 are the masses of the binary star components, a is its major semiaxis, c is the speed of light, and G is the gravitational constant. The first estimate of the gravitational-wave background from galactic binaries was obtained by Mironovskij in 1965 [115]. His estimate of the dimensional metric amplitude based on counts of W UMa binaries was $h \sim 10^{-21}$. The spectrum of the gravitational-wave background from galactic binaries was first calculated by the PS method in 1987 [116] (Fig. 6). That paper noted the presence of two different parts of the spectrum. The spectrum at low and intermediate frequencies at $\nu \sim 10^{-4}$–10^{-3} Hz is formed by binary systems whose evolution is independent of their gravitational radiation. The second part of the spectrum is formed by a high-energy tail. This tail is formed by binary systems that coalesce due to gravitational-wave emission. Binary white dwarfs mainly contribute to this part of the spectrum (at frequencies above 1 Hz, binary neutron stars).

4.9 Coalescence rates of binary neutron stars and black holes

The components of relativistic binary systems with orbital periods shorter than $\sim$ 14 h can coalesce due to the emission of gravitational waves over the Hubble time, i.e., about 10 billion years. Mergings of binary neutron stars have been widely discussed as possible sources of gamma-ray bursts and strong gravitational-wave pulses that can be detected by ground-based antennae.

The coalescence rate of binary neutron stars is the key parameter of modeling the expected gravitational-wave bursts. There are two approaches to model this rate. The first is based on the PS modeling of the evolution of binary neutron stars and the second uses the observed orbital parameters of close binary radio pulsars (similar to the famous Hulse–Taylor pulsar PSR B1913+16.) During the last 20 years, these two approaches have yielded somewhat controversial results. Starting from the first paper [116] and in all later papers (see [53] and the references therein), PS studies predicted the rate of binary neutron star coalescences of the order of 10^{-4} y^{-1} for a Milky Way-type galaxy. The estimates based on the statistics of binary pulsars gave a significantly lower coalescence rate: $\sim 10^{-6}$ y^{-1} [118]. In later papers, this value increased to 2×10^{-5} y^{-1} (see, e.g., Refs [119, 53]). The contradiction did not fully disappear at that time, however. We note that only binaries in which at least one of the components is observed as a radio pulsar are taken into account in the statistical approach, but there are other selection effects. In the PS studies, all coalescing neutron stars, including radio-silent ones, are taken into account. This difference could partially explain the divergence in the predicted rates.

In 2003, the 'double' radio pulsar J0737-3039[10] [120] increased the statistical prediction of the coalescing rate by an order of magnitude. This is related to three facts. First, the binary system has a very short orbital period, i.e., a short time before coalescence (around 85 mln y). Second, the system is located close to the Sun at the distance 600 pc. Third, both pulsars are fairly weak. Therefore, the problem of the divergence between the PS and observational estimates of binary neutron star coalescence rate is almost resolved presently [121] (Fig. 7). A short history of this problem and additional references can be found in [122]. However, there are problems related to the evolutionary formation channels for binaries like J0737-3039.

The merging rate of compact binary objects is insufficient to predict the expected detection rate of gravitational-wave signals from them. It is also necessary to know the gravitational-wave luminosity distribution of the sources. At a given sensitivity of a gravitational-wave antenna, the maximum distance from which the coalescing binary can be detected with the given ratio of signal S to noise N mainly depends on the mass of the system (more precisely, on the so-called chirp mass, which is a power-law combination of the binary mass

[10] Both components are neutron stars observed as radio pulsars.

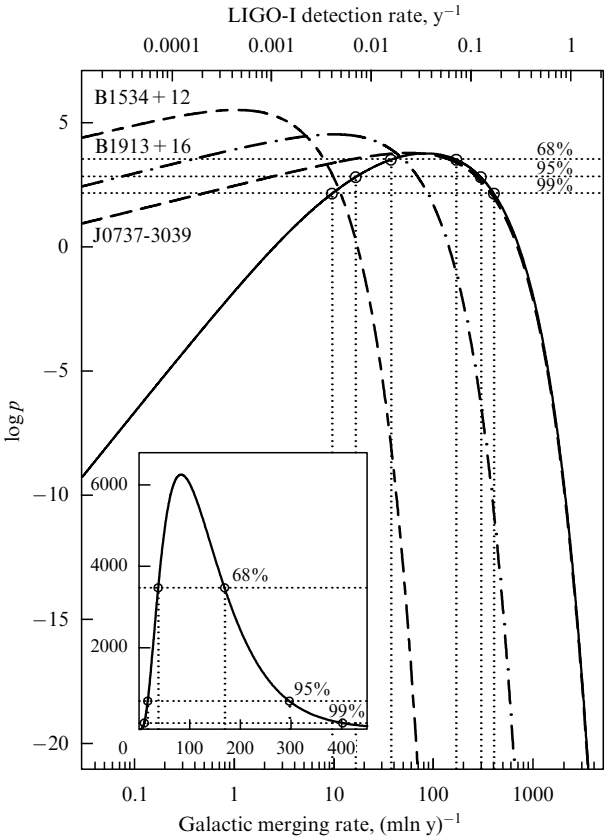

Figure 7. Estimate of the merging rate of galactic binary neutron stars based on the observations of four of the closest binary radio pulsars [121] (p is the probability density of the coalescence of binary neutron stars in the Galaxy).

components, $M_{\rm ch} = (M_1 M_2)^{3/5}(M_1 + M_2)^{-1/5}$):

$$\frac{S}{N} \propto \frac{M_{\rm ch}^{5/6}}{d}\,.$$

When ground-based interferometers reach the planned sensitivity, they will be able to detect mergings of binary neutron stars from distances of the order of several dozen Megaparsecs. The PS-predicted rate of coalescences of binary black holes is 1–2 orders of magnitude smaller than the coalescence rate of binary neutron stars, but black holes are heavier (by at least several times). Due to the strong dependence of the gravitational-wave emission power (and hence the maximum detection distance) on the mass of the binary system, the signal from binary black hole mergings must be detected from a much larger volume. We give a simple estimate, which is confirmed by PS studies. We assume that the probability of the formation of a coalescing binary neutron star from a close binary system with the initial masses of the components exceeding $10\,M_\odot$ is as high as that of merging binary black holes from systems with the initial masses of the components above $40\,M_\odot$ (although the number of the latter systems is much smaller). We also assume that the formed neutron stars (NS) and black holes (BH) have masses 1.4 and $8.5\,M_\odot$, respectively. Then the ratio of coalescence rates of binary black holes and neutron stars in a Milky Way-like galaxy is

$$\frac{R_{\rm BH}}{R_{\rm NS}} \simeq \frac{N(M > 40\,M_\odot)}{N(M > 10\,M_\odot)} = \left(\frac{40\,M_\odot}{10\,M_\odot}\right)^{-1{,}35} \simeq 0.15\,,$$

and the ratio of the detection rates of these mergings on the Earth is

$$\frac{D_{\rm BH}}{D_{\rm NS}} \simeq \left(\frac{40\,M_\odot}{10\,M_\odot}\right)^{-1.35}\left(\frac{8.5M_\odot}{1.4M_\odot}\right)^{15/6} \simeq 0.15 \times 91 \simeq 14\,.$$

Clearly, the second factor (the observed volume) turns out to be more important, and hence the expected rate of binary black hole coalescences can even be higher than that of binary neutron star mergings [123, 124]. Therefore, with high probability, the first detected signal can be from the merging of a binary black hole or a black-hole – neutron-star binary!

We note that the coalescence rate of compact binary stars significantly depends on the details of their evolution. For example, as binary black holes are formed from very massive stars with large radii, a wide binary black hole can result from the thermonuclear evolution and collapses of the components. Because the coalescence time of a binary star due to gravitational wave emission $t_{\rm GW}$ is mostly determined by the initial orbital semiaxis a_0,

$$t_{\rm GW} \propto a_0^4\,,$$

it can be much larger than the age of the Universe for such systems. In this case, the coalescence rate of binary black holes (at the present time) would be exactly zero. The situation is changed by introducing a kick velocity during black hole formation [125]. This process is quite possible if black holes are formed in a two-stage collapse (via the intermediate metastable state of a hot neutron star). Modern studies of binary black holes also support the hypothesis of a nonzero kick velocity acquired at their births [126].

4.10 Binary stars in dense stellar clusters

The evolution of the population of binary stars in dense stellar clusters (globular clusters, central dense regions of galaxies) is different from that in the galaxy field. There are two main differences: the effect of the collective nonstationary gravitational field of the cluster on individual binaries and close encounters of binary or single stars.

The interaction with the cluster gravitational field on average leads to very close (the so-called hard) binaries becoming closer and wide binaries becoming wider. The boundary between these two types of binaries is found from the condition $v_{\rm orb} \simeq v_{\rm cluster}$, where $v_{\rm orb}$ is the characteristic orbital velocity of the binary components and $v_{\rm cluster}$ is the mean velocity of cluster stars.

The close encounters lead to different possible effects (Fig. 8). The colliding star can substitute one component in a binary (the exchange, or 'recharging'), destroy the binary (dissociation), make the components coalesce, or simply change the binary orbital parameters. The probabilities of these processes were calculated in [127, 128]. A close encounter of two binary systems leads to even more diverse processes (see Refs [129, 130]).

Stellar encounters can lead to the formation of objects whose existence would be otherwise impossible, and these have the most interesting astrophysical consequences. Such objects can result from three types of processes:

• close binary collisions. The capture is due to tidal forces and is possible when the distance of the closest approach is less than 3–4 radii of the largest star. Such a close collision is very rare, but results in the formation of ultra-tight high-

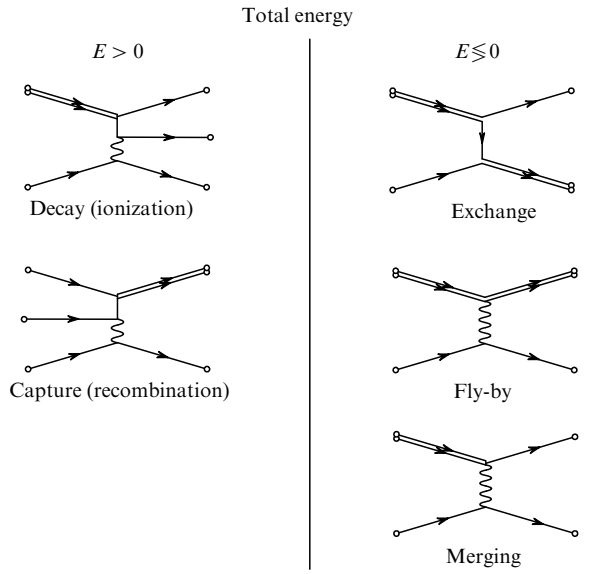

Figure 8. Possible results of a close encounter of a single star and a binary system [128].

eccentricity orbits that rapidly evolve due to gravitational-wave emission;

• close triple collisions. These result in the formation of very wide systems that are rapidly destroyed by remote encounters. The formation probability of close binaries strongly decreases with their hardness. The process is possible in the densest central parts of globular clusters and in circumnuclear regions of galaxies;

• encounters between a single and a binary star. The probability of this process is determined by the major semiaxis of the binary system. The size of the formed binary system is proportional to the major semiaxis of the initial binary. Binaries in which orbital velocities are close to the relative collision velocity are most strongly changed.

Paper [131] gives a useful simple estimate of the capture cross section of the companion for tidal interaction and exchange (the formula is most appropriate for star capture by a compact object):

$$\frac{\sigma_{\text{tidal}}}{\sigma_{\text{exch}}} = 2.5\,\frac{R_{\text{s}}}{a_0}\,,$$

where R_{s} is the radius of the captured star and a_0 is the major semiaxis of the binary system. It follows that for tidal captures, the stellar radius is the characteristic scale, while in the case of interaction with a binary it is the binary's major semiaxis. Thus, the tidal capture is usually less effective. However, the situation can be different for capture in a very tight orbit.

The attempt to take close stellar collisions (i.e., binary interactions of stars or stellar systems) into account violates one of the basic principles of PS: the independent evolution of individual objects. Nevertheless, if binary interactions are sufficiently rare, it is still possible to use PS in a somewhat modified form.

There are two possible ways of modifying the standard PS scheme to take close encounters into account. The first approach uses the full scenario of the binary star evolution and a simplified description of stellar dynamics. The second approach, in contrast, accurately accounts for stellar dynamics by using N-body calculations, and the evolutionary scenario is somewhat simplified. The second approach was used in a series of papers by Portegies Zwart, Aarseth et al. [130, 132, 133]. Of course, it is only the first step in the realization of the complete scenario of stellar evolution in dense stellar clusters.

5. Population synthesis of isolated neutron stars

In this section, we discuss the PS studies of isolated neutron stars (see review [134][11] for additional information). We focus on the following studies: radio pulsar studies, the calculation of the expected gravitational-wave signals from young neutron stars, modeling of the evolution of old neutron stars, and the study of nearby cooling (hot) neutron stars. The first two studies mainly involve modeling of the initial spin periods, velocities, and magnetic field distributions, along with the evolution of all these parameters. In addition, the angle between the magnetic moment and the spin axis can be required. The PS of cooling neutron stars uses quite different parameters. The spin period and the magnetic field only weakly affect the cooling of a neutron star, unlike its mass.

5.1 Properties of neutron stars

We first review the main facts of the astrophysics of single neutron stars (a short introduction can be found in [135]). Neutron stars result from collapses of massive stellar cores with the initial masses from approximately 8 to 30 $M_{\odot}$. The precise values of the limiting masses are poorly known. Besides, they depend on the chemical composition and, possibly, other stellar parameters. Some models predict that the evolution of the most massive stars can also end up with the formation of neutron stars because of a powerful stellar-wind mass loss [26].

The most important initial parameters of neutron stars include the spin period, the mass, the magnetic field strength, and the spatial velocity. At present, these distributions cannot be calculated theoretically and are usually inferred from observations of already strongly evolved objects by assuming some evolution of their parameters. In addition, the observed sample of objects is subjected to various selection effects. Our present knowledge of the initial parameters of neutron stars is therefore far from complete.

Spatial velocities of neutron stars are mainly determined from observations of radio pulsars. The mean velocity is found to be around 300 km s^{-1}. Maximal velocities exceed 1000 km s^{-1}. The form of the velocity distribution is poorly known (see Refs [136–138]). The reason for such high velocity, many times exceeding that of presupernovae (10–30 km s^{-1}), is apparently due to an asymmetric neutrino emission during the supernova explosion. For example, the asymmetry can be related to the convection of matter in the collapsing core or to an asymmetry of the magnetic field. However, this is quite an open issue.

The determination of masses of neutron stars is currently possible only in close binary systems. The most interesting are binary radio pulsars. To determine the initial masses of neutron stars, it is important that the star has had no time to significantly increase its mass by accretion up to the moment of observations. This requirement is satisfied for the second

[11] The electronic version is available at http://xray.sai.msu.ru/~polar/html/kniga.html.

(younger) neutron stars in double neutron star binaries. The masses of these neutron stars lie within the narrow interval $\sim 1.2-1.4\,M_\odot$. Calculations show that the initial neutron star masses can range from $1.1-1.2\,M_\odot$ up to the upper mass limit determined by the equation of state (see [139] and the references therein). However, only a few neutron stars are known to have masses in excess of $1.4-1.5\,M_\odot$. The uncertainty in calculations is due to the poorly known parameters of supernova explosions and to the possible fall-back accretion, which can increase the initial mass of a neutron star.

The initial rotation periods of neutron stars can be inferred from observations of radio pulsars with independently known ages (for example, if they are connected to historically known supernovae). Nevertheless, these estimates are model dependent, because some spin-down law has to be assumed. The magnetic dipole formula (see below) is frequently used as a simple spin-down model. The list of radio pulsars for which the initial period estimates are available can be found in [138]. The obtained values fall within a wide range from ~ 0.01 to ~ 0.14 s. Thus, neutron stars should not necessarily be formed with very short rotation periods. The initial spin periods must be determined by the following factors: the rotation period of the presupernova core, spin-up or braking due to the explosion asymmetry, rapid early spin-down due to a magnetic field, or interaction with the surrounding material. It cannot be excluded that neutron stars can be born with very long periods of about several seconds [140].

The magnetic fields of neutron stars significantly depend on presupernova fields. The field increases during the collapse due to the magnetic flux conservation [142]. In addition, the magnetic field can increase at the proto-neutron star stage, for example, by the dynamo mechanism. This mechanism is especially significant for magnetars [143]. The initial field was estimated in several papers (see below).

Once the initial parameters are determined, evolutionary laws should be specified. The evolution of neutron stars can be divided into two almost independent parts, magneto-rotational and thermal. Interaction between them is possible due to neutron star heating by the decaying magnetic field or due to rotational energy dissipation into heat. But this effect is small for most objects.

The magneto-rotational evolution includes the neutron star spin-down and the possible magnetic field decay. Details of this process are poorly known and are being actively studied now (see, e.g., Refs [140, 144, 145] and the references therein). The so-called magneto-dipole formula [146]

$$W_{\rm md} = -J\Omega\dot{\Omega} = \frac{1}{6}\,\frac{B_0^2\Omega^4 R^6}{c^3}\,\sin^2\chi$$

is commonly used. Here, $J \sim (2/5)MR^2$ is the inertia moment of the neutron star, χ is the angle between the spin axis and the magnetic dipole axis, and $\Omega = 2\pi/P$ is the spin frequency. It is easy to see that according to this formula, the spin period increases proportionally to the square root of time. However, it is obvious that the use of this formula is an oversimplification.

The magnetic field decay is also an open issue. It is determined by the neutron star crust conductivity. If the field is mostly concentrated in the core, the migration of the magnetic flux tubes from the core into the crust during the neutron star spin-down can be important. In addition, the migration of magnetic tubes is possible as the neutron star period changes, which can change the field topology (see [147] and the references therein).

The problem of neutron star cooling is extensively discussed in review [148]. A neutron star is born very hot. In 20 – 50 years, its interior temperature becomes homogeneous. Up to about 100,000 years, cooling proceeds mostly via bulk neutrino emission. Then the cooling becomes dominated by photons escaping from the surface. Recently, much progress has been made in the understanding of the thermal evolution of neutron stars [150]. However, many effects related to the cooling remain poorly studied. The main uncertainties in the theory of neutron star cooling are related to the poorly known equation of state of neutron star matter.

PS is widely used to calculate the initial parameters of neutron stars and their evolution laws. Below, we consider some examples of such an approach to different populations of objects.

5.2 Radio pulsars

Radio pulsars are the best studied and the most numerous of the observed populations of single neutron stars [144]. It is therefore not surprising that many PS studies have been done on radio pulsars. A very important feature of these studies is the need to model the *detectability* of radio pulsars, i.e., the need to not only synthesize a sample of radio pulsars but also model the actual process of their radio surveying such that the model parameters can be compared with observations. In fact, the situation is more complicated because pulsars were discovered in different surveys by different instruments, and part of them was discovered not in surveys but during some dedicated observations of specific objects (for example, supernova remnants) or fields (for example, the error boxes of gamma-ray sources).

There are three different goals of the PS studies of radio pulsars. The first is to determine the initial parameters of neutron stars (spin periods, velocities, magnetic fields). The second goal is to estimate some of their evolutionary parameters (for example, the characteristic decay time of the magnetic field). Finally, the third goal is to predict properties of so far unobserved populations of pulsars (primarily, rare and poorly studied types, such as pulsars with a very strong magnetic field and gamma-ray emitting pulsars). The population analysis of recently discovered sources that could be related to pulsars should also be mentioned.

The initial parameters of pulsars were analyzed, for example, in [136, 137], where the initial velocity distribution was studied. The recent paper [151], in which the initial pulsar periods are inferred from the analysis of the Parkes multi-beam survey, provides another example.

One of the key open issues in pulsar evolution is the neutron star magnetic field decay. Figure 9 taken from [152] shows evolutionary tracks of pulsars in the period – magnetic field diagram for single neutron stars, taking this effect into account.

Bhattacharia, Hartman, Verbunt, and Wijers devoted a series of papers to the magnetic field decay (see [6] and the references to earlier papers therein). They performed a Monte Carlo modeling of pulsar period distribution on the period – period derivative plane ($P - \dot{P}$). Simultaneously, the neutron star distribution with respect to spatial velocities, their spatial distribution, and the dispersion measure were calculated. Verbunt et al. assumed that the magnetic field distribution of neutron stars is the same as observed in radio pulsars, i.e., is

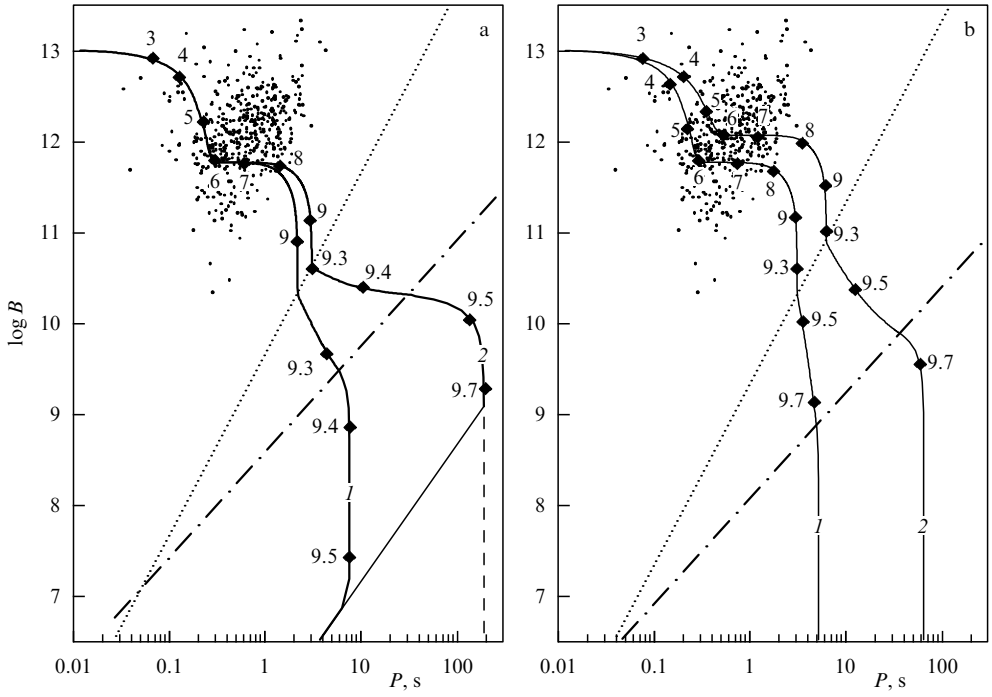

Figure 9. Evolutionary tracks of neutron stars for two models of the magnetic field decay calculated for accretion rates $\dot{M} = 10^{-15}\,M_\odot\ \mathrm{y}^{-1}$ (a) and $\dot{M} = 10^{-16} M_\odot\ \mathrm{y}^{-1}$ (b) [152]. The aim of paper [152] was to reproduce the observed parameters of the source RXJ0720.4-3125 using the model of an accreting neutron star with a decaying magnetic field. The dashed lines correspond to $p = P_\mathrm{E}$, where P_E is the critical period corresponding to the end of the ejector stage; the dashed-dotted lines show the condition $p = P_\mathrm{A}$, where P_A is the critical spin period of the neutron star at the supersonic propeller stage; below this line, accretion is possible. The tracks are marked with the logarithm of the neutron star age in years. Dots show the location of radio pulsars from the catalog by Taylor et al. [155].

Gaussian in the logarithmic scale:

$$p(\log B_i)\,\mathrm{d}\log B_i = \frac{1}{\sqrt{2\pi}\sigma_B}\exp\left[-\frac{1}{2}\left(\frac{\log B_i - \log B_0}{\sigma_B}\right)^2\right]\mathrm{d}\log B_i\,,$$

where B is the neutron star surface magnetic field. The authors used the values $\log B_0 = 12.34$ and $\sigma_B = 0.34$. They also took the detectability of each modeled source into account. Only an exponential field decay was considered: $B_i \propto \exp(-t/\tau)$. The authors concluded that the best-fit model includes the magnetic field decay on a timescale of $\tau \sim 10^8$ years with a significant part of neutron stars born with velocities below 200 km s^{-1}.

Regarding the initial parameters and the evolution, the authors have used several assumptions that can be criticized. For example, they used one-mode distributions of neutron star spatial velocities, the so-called Lyne – Lorimer distribution [153] and the Hansen – Phinney distribution:

$$\frac{4}{\pi}\frac{\mathrm{d}u}{(1+u^2)^2}\,,$$

where $u = v_i/\sigma_v$ (σ_v was set at 600 km s^{-1}). Presently, a bimodal velocity distribution is considered to be much more favorable (for example, the bi-Maxwellian distribution [136]). In addition, present observations indicate that the number of high-velocity pulsars is much larger than followed from the distribution used by Verbunt et al. The magnetic field distribution used in that paper, in principle, prohibits the existence of a noticeable fraction of magnetars. Finally, the paper by Verbunt et al. ignored the role of the angle χ between the rotation axis and the dipole magnetic moment and its evolution. Recent papers show that taking this evolution into account can be very significant (see, e.g., Refs [140, 154]).

One of the latest PS studies of pulsars was carried out in paper [149]. The authors included the evolution of the angle χ and discussed the possibility of the appearance of magnetars. The comparison of their results with the paper by Bhattacharia et al. shows the effect of the PS parameter model changing. The authors were able to bring the model into agreement with observations without introducing the magnetic field decay but assuming the evolution (increase) of the angle χ with time. The period evolution was described by the formula

$$P = P_0\left[1 + \frac{t}{\tau_0} - n_0\frac{t_\alpha}{\tau_0}\left(1 - \exp\left(-\frac{t}{t_\alpha}\right)\right)\right]^{1/2},$$

where P_0 is the initial period, t_α is the characteristic time of the angle change, and

$$\tau_0 = \frac{3}{4\pi^2}\frac{Ic^3P_0^2}{B^2R^6}\,,$$

where I is the neutron star moment of inertia and R is the neutron star radius. The parameter n_0 is related to the initial inclination angle χ_0 as $\chi_0 = \arccos\sqrt{n_0}$. The angle increase is therefore due to the increase in the energy losses, unlike the energy decrease in [144]. The possible reason for such behavior could be the motion of matter towards the neutron star poles due to a starquake [149].

Another important result in [149] is related to magnetars. The authors concluded that about 23% of neutron stars have

the magnetic field strengths $B > 10^{14}$ G. They do not assume a bimodal distribution of the magnetic fields. Magnetars naturally appeared as a high-field tail of the ordinary pulsar distribution. According to the estimates in [149], the birthrate of magnetars is one per 750 years.

Finally, a recent detailed PS study of radio pulsars is presented in [138]. The authors studied the initial radio pulsar periods, magnetic fields and kick velocities, and evolutionary effects due to the braking torque decrease. They also considered non-Maxwellian initial pulsar velocity distributions. The one-mode model with a non-Maxwellian (exponential) distribution was found to be preferential. The analytic formula for the three-dimensional velocity is quite complicated in this case. The authors of [138] write the distribution for $v_\perp$ (the transverse pulsar velocity along the plane of the Galaxy relative to the local rest frame) inferred from observations:

$$p(v_\perp) = \frac{1}{2\langle v_\perp\rangle} \exp\left(-\frac{|v_\perp|}{\langle v_\perp\rangle}\right).$$

The three-dimensional velocity turns out to be 380^{+40}_{-60} km s^{-1}. We note that the velocity distribution in [136] also provides a good fit. The authors prefer the exponential model because it is one-parameter, in contrast to the model by Arzoumanian et al., which requires two populations of pulsars with different velocity distributions (see, e.g., [156] for more details on bimodality). In constructing the global PS model of pulsars in the Galaxy, these authors used a more detailed model of the initial spatial distribution of neutron stars. Namely, they took the galactic spiral structure into account. This allowed satisfactorily describing the observed population of radio pulsars without assuming neutron star magnetic field decay or the evolution of the angle between the neutron star spin axis and the magnetic field.

Another part of radio pulsar studies is related to modeling their gamma-ray emission. Gonthier et al [157] carry out the PS of the detection process of active radio pulsars at high energies. These studies become important in the lead-up to the launch of the AGILE and GLAST missions. Gonthier et al introduced some important new parameters to describe the geometry of radio and gamma-ray fluxes. An unexpected result of their studies is a short magnetic field decay time of the order of 2.8 mln years. This result was criticized in other papers. For example, the authors of Ref. [138] argue that this could be an artifact due to the adopted model of radio luminosity. In Ref. [157], the luminosity (in units of mJy kpc^2 MHz) was given by

$$L = 3.4 \times 10^{10} P^{-1.3} \dot{P}^{0.4}.$$

In Ref. [138], the authors discuss the dependence of the observed luminosity on geometric factors and modify the model used in [157, 136] and elsewhere.

The predictions for the AGILE and GLAST observatories are very optimistic. The authors predict that GLAST can register up to 600 neutron stars in gamma rays, i.e., at least one order of magnitude larger than EGRET. We note, however, that the recent search for radio pulsars in the error boxes of unidentified EGRET sources [158] gave negative results. Apparently, predictions for GLAST and AGILE are too optimistic.

Not only active radio pulsars can be gamma-ray sources. The possibility of observing extinct radio pulsars as gamma-ray sources was studied in [159]. That paper does not use PS methods, but substantially contributes to the population models. Using analytic means, the authors constructed the distribution of 'dead' (inactive) pulsars for two models of the evolution of the angle χ between the spin axis and the magnetic dipole axis. In both models, this angle increases at the active radio pulsar stage, i.e., the star tends to become an orthogonal rotator. After the second pairs stop generating in the case of hindered particle escape, the angle starts decreasing, and the quantity $\cos\chi/P$ is conserved, where P is the neutron star spin period and χ is the angle between the magnetic and rotation axes. In the model with free particle escape from the neutron star surface, χ continues to increase and $\sin\chi/P = \text{const}$. The authors estimate the gamma-ray luminosity of the extinct radio pulsars. Apparently, modern satellites are capable of detecting such objects at distances closer than several hundreds parsecs.

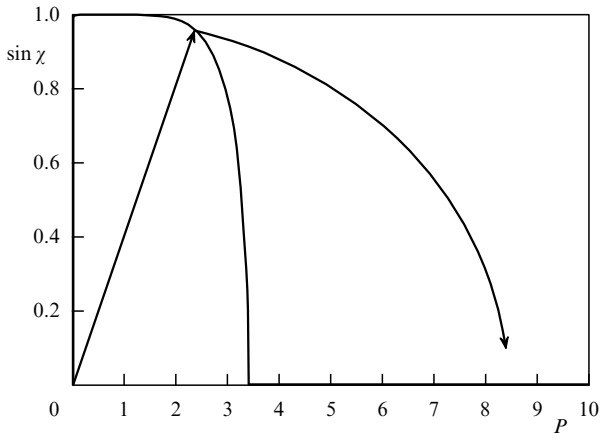

Figure 10. The reconstructed evolutionary track of the source RXJ0720.4-3125 [140]. The model of current losses [141] was used. The hindered particle escape from the neutron star surface was assumed at the extinct pulsar stage. The track corresponds to a constant field of 10^{13} G and present-day values of the spin period and the angle between the magnetic and spin axes (8.39 s and 5°). The age is found to be $\sim$ 58.4 mln years for the assumed initial spin period 20 ms.

The evolution of the angle χ can be essential for the evolution of pulsars, but many uncertainties are involved here. Figure 10, taken from [140], shows the reconstruction of the possible evolutionary track of one neutron star from the so-called 'magnificent seven' in the $\sin\chi$ – period plane. The line at which the behavior of the neutron star changes is the so-called 'death line' of radio pulsars calculated accounting for the dependence on χ. The calculation is performed for the hindered particle escape model, and therefore the angle χ starts decreasing after the pulsar crosses the death line.

As far as we know, the detailed PS of extinct radio pulsars taking the evolution of χ into account has not yet been done (although the behavior of the normal radio pulsar population has been modeled; see references in Section 2.2.7 in [134]). Such modeling can be very important because it can change our views on the state of old neutron stars, to be discussed in Section 5.4.

5.3 Estimate of the gravitational-wave signal produced by young neutron stars

The results presented below are connected with those discussed in Section 4.8. Here, we discuss the gravitational-

wave emission from young single neutron stars in more detail, taking the data in [160 – 162] into account.

Paper [160] mostly considered the gravitational-wave emission from nearby neutron stars located in the Gould belt (see also the discussion of cooling young neutron stars below). The point is that existing detectors (for example, the original VIRGO detector) can, according to estimates in [160], detect only sufficiently close (a distance below ~ 0.5 kpc) and young (an age less than $\sim 1-2$ mln y) neutron stars. However, advanced detectors can register more distant objects (the sensitivity should increase by two orders of magnitude). Hence, the contribution from the Gould belt for advanced detectors is expected to be relatively small.

For these studies, the ellipticity of the neutron star form is crucial. Several model distributions determined by the maximum entropy principle were used in [160]. In addition, the initial spin period distribution was varied.

The amplitude of the gravitational-wave signal at the frequency $f_{\rm GW} = 2/P$ (where P is the spin period) from a neutron star with a moment of inertia I and ellipticity ϵ at a distance r can be calculated from the formula

$$h_0 = 1.05 \times 10^{-27} \left(\frac{I}{1.12 \times 10^{45}\ \mathrm{g\ cm^2}}\right)\left(\frac{\epsilon}{10^{-6}}\right) \times \left(\frac{f_{\rm GW}}{100\ \mathrm{Hz}}\right)\left(\frac{10\ \mathrm{kpc}}{r}\right).$$

The sensitivity of the LIGO and VIRGO detectors at the frequency 100 Hz is then of the order of $h \sim 10^{-22}-10^{-23}$.

In our opinion, the conclusions in [160] are not too optimistic. Initial gravitational-wave interferometers have little chance of detecting gravitational radiation from nearby young neutron stars for realistic parameters. The situation will be significantly better for the advanced LIGO and VIRGO detectors. For example, for optimistic neutron star parameters, a blind search can in principle detect the gravitational-wave signal from a young neutron star located closer than 6 kpc.

The authors of [161] consider the prospects for registering the gravitational wave signal from young magnetars. Magnetars are neutron stars whose manifestations are due to the dissipation of their magnetic field (as opposed, e.g., to radio pulsars spending rotational energy, or young neutron stars radiating thermal energy). Magnetars are characterized by a strong surface magnetic field up to 10^{15} G. The internal (including toroidal) fields can be even higher.

Magnetars can be advantageous for gravitational-wave detection because a strong magnetic field misaligned with the rotation axis leads to a strong deformation of the star, making it a powerful source of gravitational waves. The magnetic-field-induced ellipticity of a neutron star can be calculated by the formula [161]

$$\epsilon_{\rm B} = g\,\frac{B^2R^4}{GM^2}\sin^2\chi = 1.9 \times 10^{-8} g B_{14}^2 R_{10}^4 M_{1.4}^{-2}\sin^2\chi\,,$$

where B, R, and M are the magnetic field, the radius, and the mass of the neutron star, χ is the angle between the magnetic and spin axes, and g is a dimensionless quantity determined by the neutron star equation of state and the magnetic field geometry.

The gravitational-wave background has been estimated for two models of the internal structure of neutron stars, leading to different ellipticities. It has been shown that at frequencies near 1 kHz, the contribution from magnetars could be higher than the cosmological (relic) gravitational-wave background.

Young magnetars are also considered in [162]. It is shown there that LIGO can detect a young magnetar up to distances of the order of 20 Mpc, i.e., sources in the Virgo cluster will be observable. The evolution of a signal in the form of frequency doubling on a timescale of one week can be a distinctive feature of a young magnetar. The frequency evolution is determined by both the electromagnetic braking ($K_{\rm d}$) and the emission of gravitational waves ($K_{\rm GW}$):

$$\dot\omega = -\frac{K_{\rm d}}{2}\,\omega^3 - \frac{K_{\rm GW}}{4}\,\omega^5\,.$$

Here, $K_{\rm GW} = (128/5)(G/c^5)I\epsilon_{\rm B}$, with I being the neutron star moment of inertia.

We note that because magnetars are expected to be located mainly in strong star-forming regions, the spatial distribution of nearby extragalactic magnetars is to be strongly inhomogeneous. Paper [163] concludes that within a few Megaparsecs, most magnetars are expected to reside in four galaxies with strong star formations: M82, M83, NGC 253, and NGC 4945 (NGC 5253 and NGC 6946 can also be mentioned). Therefore, the gravitational-wave background due to magnetars should be highly inhomogeneous.

5.4 Single neutron star counts and solitary accretors

Starting from the beginning of the 1970s, several authors have discussed the possibility of observing single accreting neutron stars. Recently, their predictions have changed from very optimistic (almost all old neutron stars are accretors; a ROSAT-class X-ray satellite should have discovered thousands of such objects) to very pessimistic (only a small fraction of old single neutron stars are at the accretion stage; most accretors are very dim sources). In the 1990s, several groups performed Monte Carlo simulations of neutron star populations. In our opinion, papers [164, 165] are two of the most significant publications.

In [164], old neutron stars are regarded as possible sources of gamma-ray bursts.[12] The PS in this paper was aimed at constructing the accreted mass distribution by single neutron stars. The accretion luminosity (erg s^{-1}) can be estimated as

$$L = \frac{\dot M G M}{R} \approx 2 \times 10^{31}\dot M_{11} M_{1.4} R_{10}^{-1}\,.$$

In turn, the accretion rate (g s^{-1}) can be evaluated as

$$\dot M = \eta\pi R_G^2 \rho v = \eta\pi\,\frac{(GM)^2}{v^3}\,\rho = \eta 10^{11} M_{1.4}^2\,\rho_{-24} v_{10}^{-3}\,,$$

where v_{10} is the neutron star spatial velocity in units 10 km s^{-1}, ρ_{-24} is the interstellar matter density in units 10^{-24} g cm^{-3}, and η is a coefficient of the order of unity. We neglect the sound velocity, because it is usually smaller than the neutron star velocity. It follows that at velocities below 100 km s^{-1}, a significant luminosity can be obtained. Most energy is to be radiated in the soft X-ray band.

The main parameters of the model used in [164] include the initial spatial distribution of neutron stars, their initial

[12] At that time, thermonuclear explosions on the surface of neutron stars located in the corona of the Galaxy were considered a viable model.

spatial velocities, the gravitational potential of the Galaxy, the interstellar matter distribution, and the type of accretion. Blaes and Rajagopal [164], as many other authors until the mid-1990s, assumed that all neutron stars relatively rapidly become accretors. This assumption is the main error of that time, because the evolution of neutron stars was completely ignored. Within this approach, all investigators obtained a great number of accreting single neutron stars.

We make a very important remark here on the evolution of single neutron stars. Until 1994, the distribution of neutron star spatial velocities predicting many low-velocity stars had been commonly accepted. After the paper by Lyne and Lorimer [153], it became clear that most neutron stars (or at least radio pulsars), in contrast, are high-velocity objects. One of the most popular spatial velocity distributions at present [136, 166] is bimodal; more than half the stars have velocities exceeding 500 – 600 km s^{-1} (however, a one-mode distribution is also supported by observations [137]). Often, different authors assume that the very small number of discovered solitary accretors [13] is explained by their low luminosities due to the high spatial velocities of neutron stars (according to the Bondi formula, the accretion rate is inversely proportional to the neutron star velocity cubed). In other words, one could say that there are many accretors, but their luminosities are too low to be detected by present-day detectors. But this is not the case! Neutron stars with such high spatial velocities never become accretors. Most of their lives are spent at the ejector stage and then they become georotators (see below); the propeller stage could also be important [167]. Hence, the number of single accretors is mainly determined by the fraction of low-velocity neutron stars.

The duration of stages preceding the accretion stage was discussed in [165]. The approach in that paper is in some sense intermediate. On the one hand, the authors did not use a new spatial velocity distribution (according to Lyne and Lorimer). Therefore, a notable fraction of neutron stars become accretors over the Galaxy's lifetime. On the other hand, the authors took the evolution of neutron stars into account (in a very simplified form) before the accretion stage, which makes this study much more advanced than most other models up to the end of the 1990s.

An attempt to carry out a global PS study of single neutron stars was made in Ref. [168]. This 'census' of neutron stars was performed to determine fractions of the neutron star populations at each of the four main evolutionary stages: the ejector, the propeller, the accretor, and the georotator (a description of these stages is given in Ref. [10]). From the modern standpoint, this study has several shortcomings. The authors used very simple initial distributions for rotation periods and magnetic fields and a one-mode velocity distribution. The propeller and georotator stage were described in a simplified way, and the evolution of the rotator inclination angle χ was completely ignored. In spite of this, in our opinion, the main features of the real distribution of neutron stars are correctly described in that paper. For the standard magnetic field distribution (without decay), neutron stars spend most of their lives as ejectors (or as georotators for high-velocity objects). This follows from the expression for the duration of the ejector stage (in years):

$$t_{\rm E} \sim 10^9 \mu_{30}^{-1} n^{-1/2} v_{10} \,.$$

[13] Currently, no source is definitely identified as a single accreting neutron star.

Here, n is the number density of interstellar matter particles and μ_{30} is the magnetic moment in units 10^{30} G cm^3.

When field decay is present, neutron stars at the propeller stage can be the most numerous. The spin-down of a neutron star at the supersonic propeller stage is poorly known (see the list of formulas, e.g., in Ref. [169]). In one of the models (see [168]), we have

$$t_{\rm P} \sim 10^6 \mu_{30}^{-8/7} n^{-3/7} v_{10}^{9/7}$$

(the time is expressed in years). Hence, for magnetic fields $\lesssim 10^9$ G, the lifetime at the supersonic propeller stage becomes very long.

Paper [168] shows that for a reasonable velocity distribution, more than 90% of single neutron stars should never leave the ejector stage, and the fractions of propellers and georotators are small. In that paper, the beginning of the georotator stage is oversimplified. This stage follows the ejector stage if the gravimagnetic parameter $y = \dot{M}/\mu^2$ is very small (see [170] for a detailed description of these stages). It is required that the gravitational capture radius be smaller than the magnetosphere radius. Then the effects of gravity are small (for the terrestrial magnetosphere). The corresponding condition can be written as [168]

$$v > 410\, n^{1/10} \mu_{30}^{-1/5}$$

(where v is measured in km s^{-1}).

We note that the three formulas above are not very robust. First, they are model-dependent. Second, the numerical coefficients are known to an accuracy of several dozen per cent because of the approximate character of the initial expressions used for their derivation. Nevertheless, they give order-of-magnitude estimates and show the 'general trend' in the evolution of single neutron stars.

In Ref. [168], the end of the ejector stage was determined only by the condition of the capture radius exceeding that of the light cylinder. The reverse situation is important for high-velocity neutron stars. In the correct description, most high-velocity ejectors should actually become georotators. The supersonic propeller stage was also ignored (see [167] and the references therein).

A more detailed study of the properties of single accreting neutron stars was carried out in [171]. The authors constructed a $\log N - \log S$ distribution for accretors. They showed that at small X-ray fluxes (below 10^{-13} – 10^{-14} erg s^{-1} cm^{-2}), accretors become more numerous than young cooling neutron stars (these sources are described in more detail in the next section). In addition, the authors calculated velocities, temperatures, and accretion rates of single accreting neutron stars.

In conclusion, we note once again that the PS studies of old single neutron stars have come a long way. Many elements of their evolutionary scenario have been considerably amended. Nevertheless, many details of the magneto-rotational evolution of neutron stars remain unclear (the evolution of the angle χ, properties of the propeller stage, the rate and efficiency of accretion, etc.). Hence, more detailed PS studies will inevitably be carried out in the future.

5.5 Nearby young neutron stars

Another field of neutron star population studies is the study of nearby young cooling neutron stars. The ROSAT satellite

has discovered more than ten hot neutron stars of different types in the solar vicinity (see the list in [172]). They include four normal radio pulsars, Geminga and one similar source, and seven radio-quiet neutron stars (the so-called 'magnificent seven'). Of course, the list is incomplete: more neutron stars are expected to lurk in the solar vicinity. However, it is difficult to identify such sources in the galactic plane. These sources can be considered homogeneous, because all of them were detected by one instrument, and there is an upper distance from which these sources can be detected (due to the strong absorption of soft X-rays by interstellar matter). The homogeneity of the sampling is very useful for PS studies, because the sources suffer from the same selection effects of the detection procedure itself.

The purpose of such a study can be twofold: to understand the nature of the observed sampling of sources and to check whether their observational properties can be explained by theoretical cooling curves. The first issue was studied in [172-174] and the second problem was investigated in [175].

For the PS study of this sampling of sources, it is necessary to determine the following relations:

- the initial spatial distribution of neutron stars (or their massive-star progenitors);
- the initial spatial velocity distribution;
- the mass spectrum of neutron stars;
- cooling curves;
- the emitting spectrum of neutron stars;
- properties of interstellar matter (to account for absorption);
- parameters of the detector that registered these neutron stars.

Some of these properties (for example, the spatial velocity distribution or the local interstellar medium structure) are known fairly well because they were studied independently in relation to other problems, but others are much less known. For example, the neutron star mass spectrum, which is very important in this study, is poorly known; in Refs [173, 175], the mass spectrum was estimated based on observations of massive stars in the solar vicinity and calculations of massive star evolutions. In the solar vicinity, a small fraction of young neutron stars with a mass exceeding $\sim 1.4-1.5\,M_{\odot}$ was found.

It was shown in [172] that the local population of hot neutron stars from which thermal radiation was observed is generically related to the Gould belt. The Gould belt is the local structure characterized by an increased number of massive stars (and correspondingly of young compact objects) in the solar vicinity (see, e.g., Ref. [174]). The use of the distribution $\log N - \log S$ as an independent additional test of the thermal evolution of neutron stars was suggested in [175].

Presently, the theoretical description of the thermal evolution of neutron stars is compared with observations using the so-called $T - t$ (temperature–age) diagram. This test, which is the most natural one, has some shortcomings:

- there are uncertainties in the temperatures and ages of individual neutron stars because both parameters are inferred from observations;
- the test has a low sensitivity to neutron stars with ages above 100 thousand years;
- the test uses an inhomogeneous sample of sources (neutron stars of different types).

The relation $\log N - \log S$ successfully adds to the test $T - t$:

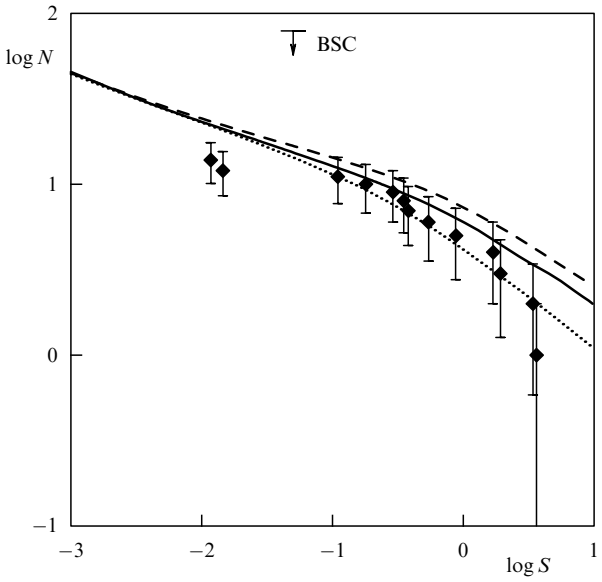

Figure 11. The $\log N - \log S$ distribution for nearby cooling neutron stars. The diamonds show the observed objects. The error bars correspond to the Poisson distribution. The curves were calculated by the PS method for hybrid stars (model 4 in [176]). The curves correspond to different initial distributions of neutron stars. The lower and upper curves are calculated for a simplified model in which the Gould belt is represented by a flat disk with the respective radius 500 and 300 pc. The middle curve corresponds to a more realistic distribution of stars based on observations of massive stars in the solar vicinity. BSC corresponds to an upper limit of the possible number of unidentified sources of this type in the ROSAT Bright Source Catalogue [177].

- only directly observed quantities are used (i.e., observational uncertainties are smaller);
- the observed sampling of sources is homogeneous (all neutron stars belong to the synthesized population);
- the test is most sensitive for neutron stars with ages above several hundred thousand years.

On the other hand, the $\log N - \log S$ test has its own shortcomings (see [175] for more details).

Preliminary results indicate that the $\log N - \log S$ test is complementary to the standard $T - t$ test (i.e., these tests should be combined; the use of only the $\log N - \log S$ test is much less informative). This is a good example of how the astrophysical PS can be applied to study properties of matter under extreme conditions.

Figure 11 shows $\log N - \log S$ distributions for nearby cooling neutron stars detected by the ROSAT satellite. The curves correspond to different initial distributions of neutron stars. Figure 12 presents the map of a model distribution of isolated cooling neutron stars near the Sun registered by the ROSAT satellites at the flux level of more than 0.05 counts per second. The sources are seen to concentrate toward the galactic plane and the Gould belt, as well as toward several nearby associations and clusters of massive stars.

5.6 Unsolved problems

Unfortunately, many aspects of the PS models presented above are poorly known.

In our opinion, the main difficulties of the PS studies of radio pulsars are due to an incomplete understanding of the emission mechanisms of these objects at different energies. This makes it difficult to determine critical model parameters and to obtain results that can be directly compared with

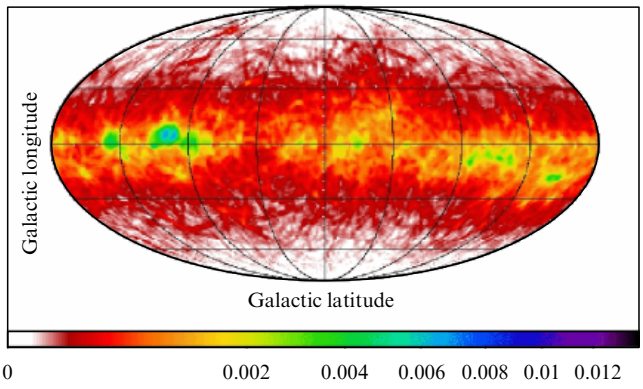

Figure 12. A model calculation of cooling neutron stars. Galactic coordinates are used. Individual tracks of neutron stars are seen at high galactic latitudes. A realistic initial spatial distribution of neutron stars was used. The enhanced density near the galactic plane and the Gould belt corresponds to nearby rich clusters and associations of massive stars [178].

observations. Many authors have obtained very different results using the same model parameters but different emission mechanisms. We repeat here that the initial magnetic fields and spin periods, as well as the evolution of the angle between the magnetic and spin axes, are not known very well.

A detailed PS study of magnetars has not yet been performed because of poor statistics. Only four soft gamma-ray repeaters (SGRs) and around ten anomalous X-ray pulsars are currently known. Observations of giant outbursts from SGRs in nearby large galaxies should allow further progress here.

The PS studies of old neutron stars also suffer from insufficient statistics. Presently, no old isolated neutron star that is not a millisecond pulsar is definitely known. The probability of finding some means to discover isolated neutron stars at the propeller or georotator stage is extremely small. To the theoretical uncertainties discussed above, we should add problems with describing the propeller stage. The efficiency of accretion onto a neutron star is also poorly known (in comparison with the Bondi formula, which can be considered a theoretical upper limit; see Ref. [179]).

Uncertainties in the mass spectrum of neutron stars and in light curves and their emission properties (spectra and the radiation capacity of the surface) affect calculations of cooling young neutron stars. All these parameters are actively being studied at present, and therefore, hopefully, some progress in the PS studies of isolated neutron stars will be made in the next several years.

6. Other examples of population synthesis

6.1 Stellar populations and spectral studies

PS studies of stellar populations started at the end of the 1960s to the beginning of the 1970s (see the references to early papers and a short historical introduction in Refs [4, 5]).

Historically, *empirical PS* appeared earlier than *evolutionary PS*. Presently, both these methods are widely used (see [4] for more details on evolutionary population synthesis and references). Empirical PS is described in detail in [2]. Both methods are discussed in [1].

The need to elaborate these methods was dictated by the same problem: to infer properties of the stellar population (age, chemical composition, etc.) from the integral spectrum of a galaxy; the inverse problem can also be formulated: to obtain the model galaxy spectrum from an analysis of its stellar populations. Resolution of individual stellar populations in a galaxy has so far been possible only for nearby galaxies located closer than ~ 1 Mpc [180], i.e., mainly for dwarf galaxies from the Local group.

Empirical population synthesis is based on the *decomposition* of the spectrum of a galaxy into the known spectra from different stellar populations. The solution to this problem is to find a linear combination of stellar spectra that best fit the integral spectrum of the galaxy (the equivalent width of spectral lines are very often used in this approximation). The main difficulty of this method is the degeneracy of the decomposition leading to free parameters and the nonuniqueness of the decomposition. For example, a change in metallicity alters the spectrum of a stellar population in the same way as a change in its age: increasing metallicity and age make the spectrum of the population redder (see the discussion in [181]).

Evolutionary PS requires knowledge of:

- the initial mass function;
- the rate and history of star formation;
- the initial chemical composition and the rate of elemental enrichment of the medium.

The main problems here are related to our insufficient knowledge of the stellar evolution (first and foremost, after the main sequence) [3, 182]. In addition, there is a degeneracy in the dependence on the initial mass function: for example, a fractional change of the massive star number yields the same spectral effect as a change in the age of the entire population (this problem emerges in the age determination of stellar populations with star formation bursts; see the discussion in [183]).

Both methods use similar initial information. Evolutionary PS uses stellar spectra that depend on the chemical composition, the surface gravity, and the effective temperature. Empirical PS uses spectra of typical stellar populations, for example, the integral spectrum of a sample of stars with the same age and initial chemical composition. In this method, the observed spectrum of a galaxy is approximated by combining spectra of samples with different ages.

To calculate the integral spectra, it is important to have a set (library) of parameters of stars and their populations (see Ref. [184]). It is very important to calculate the so-called *isochrones* — the set of parameters of a stellar population with a certain age, which is related to the possibility of subdividing any population into subpopulations resulting from an instantaneous star-formation burst. The task becomes more difficult because of the need to take different chemical compositions, binary systems, and other facts into account (see the original results and references in [3, 4]).

Rapid rotation can be an additional parameter. It is especially important for massive stars [185]. Based on evolutionary tracks calculated by the Geneva group [186], the authors of [187] considered the PS model of massive stars.

Taking rotation into account increases the luminosity for a given stellar mass. Therefore, first, the determination of the mass from the luminosity using nonrotational models leads to its overestimation. Second, the rotation of main-sequence stars with a mass below 30 $M_\odot$ leads to the formation of more massive helium cores. Finally, rotating stars spend more time

in the main sequence. This changes the properties of the entire population. The population with rotation turns out to be brighter and bluer than the nonrotational one. It is therefore possible that some estimates of the mass of populations from their total luminosity and the initial mass function determination can be changed in the future.

For a long time, the PS studies of normal stars had been carried out ignoring the presence of binary stars. Only at the end of the 1990s did some authors start including binary stars in the model (see [188] and the references therein). Recent results can be found in [189, 190] and in review [191].

All authors concluded that the effects of binary stars on the integral optical spectrum are very important. For example, small-mass Wolf – Rayet stars (helium stars) can be formed mainly in binaries (massive Wolf – Rayet stars can also result from the most massive single stars if a very strong stellar wind is assumed). In addition, binary systems are 'factories' producing stars such as blue strugglers, B-subdwarfs (sdB's), and Be-stars (see the recent discussion in [192]).

Paper [189] shows that the evolutionary effects in binaries make the color indices of a population bluer. The study of high-resolution spectral indices [190] revealed that the dependence is more complicated: some of them turn out to be redder than the color indexes, some of them bluer. The effect is determined by the age and metallicity.

Another specific PS problem is related to galaxies with a high star-formation rate [193]. Modeling of recent star formation bursts is a complicated task for the following reasons:

- the difficulty in calculating the integral spectra due to the large number of massive stars;
- stars in the burst not being born simultaneously;
- nonhomogeneity of the interstellar medium and the presence of dust.

A detailed age determination of young star formation bursts is carried out in [183]. The model used in that paper includes the population of single stars with several star formation bursts. To determine the age of individual bursts, the widths of spectral lines (or other features) are used. For example, to single out the youngest star formation bursts (~ 4 mln years), nebular emission lines and ultraviolet lines connected to the stellar wind are used.

It is essential that star formation bursts strongly influence the integral spectra of galaxies. The results of a detailed study were recently presented in [194]. At small redshifts, even a moderate burst makes the galaxy spectrum much bluer. At high redshifts, where galaxies are fairly young, this effect is much less pronounced. After a short stage (several million years) during which stars born in the star formation burst are bluer, a longer stage begins at which evolved young stars make the spectrum redder. This stage can last as long as a few billion years. Even without taking the contribution from dust into account, the post-burst reddening may explain the spectra of so-called extremely red objects (EROs). Therefore, the authors of [194] suggest a third alternative for the nature of these red galaxies (in addition to ideas that either these galaxies have a low star formation rate, i.e., are passive galaxies, or they are star-forming galaxies with very big dust content).

Examples of the age determinations of old stellar populations and references can be found in [181]. In that paper, the authors applied the model of one stellar population to the galaxy M32 (a satellite of the Andromeda galaxy) and obtained agreement with observations assuming the age ~ 6.5 bln years and the solar chemical composition.

Paper [192] used the evolutionary PS to calculate an important galactic characteristic — the mass-to-luminosity ratio (M/L). This ratio is widely used to evaluate the mass of a galaxy by its luminosity in some band.

6.2 Active galactic nuclei and X-ray background

Observations by the Einstein, ROSAT, XMM, and especially the Chandra satellites showed that more than 60% of the X-ray background (up to 90% in the soft X-ray band) can be resolved into individual sources; in other words, point-like objects and not a diffusive background are responsible for this emission. The optical identification of resolved sources indicates that most of them are active galactic nuclei (AGNs) and others are explained by galaxy clusters and individual stars.

These observations have raised the interest in PS studies of AGNs. First, PS models of the X-ray background were based on the so-called unified model of active nuclei (papers [196, 197] give examples of such calculations and references to earlier works). In this model, all manifestations of the AGN activity are explained by accretion onto the central supermassive black hole (see [198] for a description of the unified AGN model). Different AGN types appear because of the central black hole mass difference, properties of the accreting matter, and especially the formation of a torus around the central black hole. In addition, a different orientation of the torus with respect to the terrestrial observer results in different activity manifestations. Later on, the PS models became more phenomenological and accounted for much of the observational data (see, e.g., Refs [199 – 203]).

The main components of the AGN PS are as follows:

- the relative fraction of nuclei screened (large absorption) and unscreened by tori;
- the AGN luminosity function;
- the spectral energy distribution;
- the evolution of the above parameters (if there are any such parameters).

Usually, these models are closer to 'population synthesis' in the definition used in [1] than to scenarios described in Sections 4 and 5 (which are called 'evolutionary synthesis' in [1]). In the X-ray background studies, the authors did not follow the evolution of an AGN from some initial state (for example, from the appearance of the central black hole or even earlier, from the beginning of the process of hierarchical clustering of galaxies). In most papers, the background was presented as a sum of contributions from unabsorbed (i.e., unscreened by tori, the so-called type 1) and absorbed (type 2) AGNs. The type-2 AGN spectra can be calculated from type-1 spectra by introducing some absorption. This is the leading contribution of the unified AGN model to PS. Early works used the ratio of type-1 to type-2 AGNs as predicted by the unified model (roughly, 1:4); now the observed ratio is more often used (typically, from 3.7:1 to 3:1).

A modification of the unified model was proposed in [202]. The original unified model assumes a single geometric structure for all AGNs, which is independent of both the luminosity and redshift. The authors of [202] point out that the fraction of active galactic nuclei with strong absorption decreases with increasing the luminosity. This result is obtained from the analysis of the HEAO1, ASCA, and Chandra data for 247 sources. Using this modification, the

authors calculate a population model for the X-ray background.

Another modification is proposed in [203]. The authors argue that the intrinsic absorption in active galactic nuclei strongly evolves with redshift. It is important that according to the conclusion by these authors, the evolution of type-1 and type-2 active galactic nuclei are different. It is possible, however, that the conclusion on the significant evolution with redshift is preliminary and more observations are required (especially with the infrared Spitzer space telescope [204]).

Presently, such models provide a sufficiently successful explanation of X-ray background properties. In spite of this, the input parameters of the used models must be made less phenomenological. This can be done by connecting the PS AGN studies with calculations of earlier stages of the evolution of galaxies (protogalaxy mergings, the appearance of the central black hole, etc.), which provide the initial conditions for the PS calculations. It is also necessary to account for the contribution from star formation bursts to the X-ray background (see [201]).

7. Conclusion

In this review, we briefly described the main applications of the *population synthesis* method in astrophysics. These applications are related to various observations: from normal stars to compact objects, from the integral spectra of galaxies to the X-ray background. The main focus was on PS calculations of single and binary neutron stars, because these problems are close to the fields of the authors' interests.

Population synthesis as a method of theoretical (numerical) study is a typical astrophysical tool, because we very frequently observe only a small fraction of the source population or cannot resolve individual sources at all. In these cases, population synthesis can significantly help in determining parameters of the entire population or in verifying parameters obtained by different means, as well as in predicting properties of so far unobserved objects.

As knowledge on the studied population increases, the PS models become more and more complicated. However, when all objects of the population become observable and their evolution can be derived directly from experimental data, the PS method becomes useless (with the possible exception of checking the self-consistency of the obtained results). Unfortunately (or luckily), we are too far from such an ideal in most astrophysical situations, and therefore population synthesis will remain an important astrophysical tool for a long time.

This review was partially supported by the RFBR grant 06-02-16205. S B Popov acknowledges INTAS and the Dynasty Foundation for support.

References

1. Fritze-v. Alvensleben U, in *Stars, Gas, and Dust in Galaxies: Exploring the Links* (ASP Conf. Ser., Vol. 221, Eds D Alloin, K Olsen, G Galaz) (San Francisco, Calif.: Astron. Soc. of the Pacific, 2000) p. 179; astro-ph/0009290
2. Cid Fernandes R et al. *Mon. Not. R. Astron. Soc.* **325** 60 (2001)
3. Maraston C *Mon. Not. R. Astron. Soc.* **362** 799 (2005)
4. Bruzual G, Charlot S *Mon. Not. R. Astron. Soc.* **344** 1000 (2003)
5. Maraston C, in *Extragalactic Globular Cluster Systems* (ESO Astrophys. Symp., Ed. M Kissler-Patig) (Berlin: Springer, 2003) p. 237; astro-ph/0301419
6. Verbunt F et al., in *Pulsar Timing, General Relativity, and the Internal Structure of Neutron Stars* (Eds Z Arzoumanian, F van der Hooft, E P J van den Heuvel) (Amsterdam: Royal Netherlands Acad. of Arts and Sci., 1999) p. 215
7. Cerviño M, Valls-Gabaud D *Mon. Not. R. Astron. Soc.* **338** 481 (2003)
8. Cerviño M, Luridiana V *Astron. Astrophys.* **413** 145 (2004)
9. Cerviño M, Luridiana V, astro-ph/0510411
10. Lipunov V M, Postnov K A, Prokhorov M E *Astrophys. Space Sci. Rev.* **9** 1 (1996)
11. Taam R E, Sandquist E L *Annu. Rev. Astron. Astrophys.* **38** 113 (2000)
12. Webbink R F *Astrophys. J.* **227** 355 (1984)
13. de Kool M *Astrophys. J.* **358** 189 (1990)
14. Nelemans G et al. *Astron. Astrophys.* **360** 1011 (2000)
15. Bisnovatyi-Kogan G S *Fizicheskie Voprosy Teorii Zvezdnoi Evolyutsii* (Moscow: Nauka, 1989) [Translated into English: *Stellar Physics* Vol. 1, 2 (Berlin: Springer, 2001 – 2002)]
16. Shapiro S L, Teukolsky S A *Black Holes, White Dwarfs, and Neutron Stars* (New York: Wiley-Interscience, 1983) [Translated into Russian (Moscow: Mir, 1985)]
17. Lipunov V M et al., arXiv:0704.1387
18. Vanbeveren D, De Loore C, van Rensbergen W *Astron. Astrophys. Rev.* **9** 63 (1998); Vanbeveren D, van Rensbergen W, de Loore C *The Brightest Binaries* (Astrophysics and Space Science Library, Vol. 232) (Dordrecht: Kluwer Acad. Publ., 1998)
19. Salasnich B, Bressan A, Chiosi C *Astron. Astrophys.* **342** 131 (1999)
20. Yungelson L R, in *Interacting Binaries: Accretion, Evolution, Outcomes* (AIP Conf. Proc., Vol. 797, Eds L Burderiet et al.) (Melville, NY: AIP, 2005) p. 1
21. Postnov K A, Yungelson L R *Living Rev. Relat.* **9** 6 (2006)
22. Mannings V, Boss A P, Russell S S (Eds) *Protostars and Planets IV* (Tucson: Univ. of Arizona Press, 2000)
23. Reipurth B, Jewitt D, Keil K (Eds) *Protostars and Planets V* (Tucson: Univ. of Arizona Press, 2007)
24. Surdin V G *Rozhdenie Zvezd* (Birth of Stars) (Moscow: Editorial URSS, 2000)
25. Lejeune T, Schaerer D *Astron. Astrophys.* **366** 538 (2001)
26. Woosley S E, Heger A, Weaver T A *Rev. Mod. Phys.* **74** 1015 (2002)
27. Roche lobe, http://en.wikipedia.org/wiki/Roche_lobe
28. Kornilov V G, Lipunov V M *Astron. Zh.* **60** 284, 574 (1983) [*Sov. Astron.* **27** 163, 334 (1983)]
29. Dewey R J, Cordes J M *Astrophys. J.* **321** 780 (1987)
30. Paczyński B *Annu. Rev. Astron. Astrophys.* **9** 183 (1971)
31. van den Heuvel E P J, in *Neutron Stars: Theory and Observation* (NATO ASI Series. Ser. C, No. 344, Eds J Ventura, D Pines) (Dordrecht: Kluwer Acad. Publ., 1991) p. 171
32. Panchenko I E et al. *Astron. Astrophys. Suppl. Ser.* **138** 517 (1999)
33. Lipunov V M, Panchenko I E, in *The Astrophysics of Gravitational Wave Sources* (AIP Conf. Proc., Vol. 686, Ed. J M Centrella) (Melville, NY: AIP, 2003) p. 285
34. Popov S B, Prokhorov M E *Astron. Astrophys.* **434** 649 (2005)
35. Bogomazov A I, Abubekerov M K, Lipunov V M *Astron. Zh.* **82** 722 (2005) [*Astron. Rep.* **49** 644 (2005)]
36. Yungelson L R, in *White Dwarfs: Cosmological and Galactic Probes* (Astrophysics and Space Science Library, Vol. 332, Eds E M Sion, S Vennes, H L Shipman) (Dordrecht: Springer, 2005) p. 163
37. Napiwotzki R et al., in *14th European Workshop on White Dwarfs* (ASP Conf. Ser., Vol. 334, Eds D Koester, S Moehler) (San Francisco, Calif.: Astron. Soc. of the Pacific, 2005) p. 375
38. Yungel'son L R, Tutukov A V *Astron. Zh.* **82** 976 (2005) [*Astron. Rep.* **49** 871 (2005)]
39. Nelemans G, Yungelson L R, Portegies Zwart S F *Mon. Not. R. Astron. Soc.* **349** 181 (2004)
40. Pols O R, Marinus M *Astron. Astrophys.* **288** 475 (1994)
41. Hurley J R, Tout C A, Pols O R *Mon. Not. R. Astron. Soc.* **329** 897 (2002)
42. Sills A et al. *New Astron.* **8** 605 (2003)
43. Muno M P et al. *Astrophys. J.* **636** L41 (2006)
44. Portegies Zwart S F et al. *Mon. Not. R. Astron. Soc.* **351** 473 (2004)
45. Portegies Zwart S F, Dewi J, Maccarone T *Mon. Not. R. Astron. Soc.* **355** 413 (2004)
46. Portegies Zwart S F, astro-ph/0406550

47. Portegies Zwart S F, Verbunt F *Astron. Astrophys.* **309** 179 (1996)
48. Podsiadlowski Ph et al. *Astrophys. J.* **612** 1044 (2004)
49. Dewi J D M, Podsiadlowski Ph, Pols O R *Mon. Not. R. Astron. Soc.* **363** L71 (2005)
50. Dewi J D M, Podsiadlowski Ph, Sena A *Mon. Not. R. Astron. Soc.* **368** 1742 (2006)
51. Podsiadlowski Ph et al. *Astrophys. J.* **607** L17 (2004)
52. Han Z et al., in *Evolution of Binary and Multiple Systems* (ASP Conf. Ser., Vol. 229, Eds P Podsiadlowski et al.) (San Francisco, Calif.: Astron. Soc. of the Pacific, 2001) p. 205
53. Kim C, Kalogera V, Lorimer D R *Astrophys. J.* **584** 985 (2003)
54. Kalogera V et al., in *Binary Radio Pulsars* (ASP Conf. Ser., Vol. 328, Eds F A Rasio, I H Stairs) (San Francisco, Calif.: Astron. Soc. of the Pacific, 2005) p. 261
55. Fryer C L, Kalogera V *Astrophys. J.* **554** 548 (2001)
56. Willems B, Kalogera V *Astrophys. J.* **603** L101 (2004)
57. Belczynski K et al., astro-ph/0511811
58. Kalogera V et al. *Phys. Rep.* **442** 75 (2007); astro-ph/0612144
59. Willems B, Mundin R P, Kolb U, in *The Physics of Cataclysmic Variables and Related Objects* (ASP Conf. Ser., Vol. 261, Eds B T Gänsicke, K Beuermann, R Reinsch) (San Francisco, Calif.: Astron. Soc. of the Pacific, 2002) p. 303
60. Willems B, Kolb U *Mon. Not. R. Astron. Soc.* **337** 1004 (2002); *Astron. Astrophys.* **419** 1057 (2004)
61. Willems B, Kolb U *Astron. Nachr.* **324** 169 (2003); in *Binary Radio Pulsars* (ASP Conf. Ser., Vol. 328, Eds F A Rasio, I H Stairs) (San Francisco, Calif.: Astron. Soc. of the Pacific, 2005) p. 255
62. Tutukov A V, Yungel'son L R *Astron. Zh.* **79** 738 (2002) [*Astron. Rep.* **46** 667 (2002)]
63. Fedorova A V, Tutukov A V, Yungel'son L R *Pis'ma Astron. Zh.* **30** 92 (2004) [*Astron. Lett.* **30** 73 (2004)]
64. Lü G, Yungelson L, Han Z *Mon. Not. R. Astron. Soc.* **372** 1389 (2006)
65. Belczynski K, Bulik T, Kluźniak W *Astrophys. J.* **567** L63 (2002)
66. Kolb U, in *Wild Stars in the Old West* (ASP Conf. Ser., Vol. 137, Eds S Howell, E Kuulkers, C Woodward) (San Francisco, Calif.: Astron. Soc. of the Pacific, 1998) p. 190
67. Kolb U, King A R, Ritter H *Mon. Not. R. Astron. Soc.* **298** L29 (1998)
68. Howell S B, Nelson L A, Rappaport S *Astrophys. J.* **550** 897 (2001)
69. Willems B, Kolb U *Astron. Astrophys.* **419** 1057 (2004)
70. Kolb U, Willems B *Rev. Mex. Astron. Astrofís.* **20** 101 (2004)
71. Nelemans G, Tout C A *Mon. Not. R. Astron. Soc.* **356** 753 (2005)
72. van der Sluys M V, Verbunt F, Pols O R *Astron. Astrophys.* **460** 209 (2006)
73. Iben I (Jr.), Tutukov A V, Yungelson L R *Astrophys. J.* **475** 291 (1997)
74. Nelemans G, Tout C A *Rev. Mex. Astron. Astrofís.* **20** 39 (2004)
75. Politano M *Am. Astron. Soc. Meeting* **199** 62.08 (2001); *Bull. Am. Astron. Soc.* **33** 1401 (2001)
76. Politano M *Astrophys. J.* **604** 817 (2004)
77. Politano M, Weiler K P, astro-ph/0702662
78. Nelemans G et al. *Astron. Astrophys.* **365** 491 (2001)
79. Mannucci F et al. *Astron. Astrophys.* **433** 807 (2005)
80. van der Kliss M *Annu. Rev. Astron. Astrophys.* **38** 717 (2000)
81. Swank J, Markwardt C, in *New Century of X-ray Astronomy* (ASP Conf. Ser., Vol. 251, Eds H Inoue, H Kunieda) (San Francisco, Calif.: Astron. Soc. of the Pacific, 2001) p. 94
82. Grimm H-J, Gilfanov M, Sunyaev R *Memorie Della Soc. Astron. Italiana* **73** 1053 (2002)
83. Smale A P, Homan J, Kuulkers E *Astrophys. J.* **590** 1035 (2003)
84. Podsiadlowski Ph, Rappaport S, Pfahl E, in *The Influence of Binaries on Stellar Population Studies* (Astrophysics and Space Science Library, Vol. 264, Ed. D Vanbeveren) (Dordrecht: Kluwer Acad. Publ., 2001) p. 355
85. Pfahl E, Rappaport S, Podsiadlowski Ph *Astrophys. J.* **597** 1036 (2003)
86. Raguzova N V *Astron. Astrophys.* **367** 848 (2001); *Astrophys. Space Sci.* **281** 641 (2002); Raguzova N V, Shugarov S Yu, Ketsaris N A *Astron. Zh.* **80** 535 (2003) [*Astron. Rep.* **80** 535 (2003)]
87. Zezas A, Chandra Proposal No. 07620901 (2005)
88. Liu X-W, Li X-D *Astron. Astrophys.* **449** 135 (2006)
89. Ruiter A J, Belczynski K, Harrison T E *Astrophys. J. Lett.* **640** 167 (2006)
90. Story S A, Gonthier P L, Harding A K *Am. Astron. Soc. Meeting* **207** 183.10 (2006)
91. Willems B, Kolb U, in *Binary Radio Pulsars* (ASP Conf. Ser., Vol. 328, Eds F A Rasio, I H Stairs) (San Francisco, Calif.: Astron. Soc. of the Pacific, 2005) p. 255
92. Eggleton P P, Verbunt F *Mon. Not. R. Astron. Soc.* **220** 13P (1986)
93. Mardling R, Aarseth S, in *The Dynamics of Small Bodies in the Solar System, A Major Key to Solar System Studies* (NATO ASI Series. Ser. C, No. 522, Eds B A Steves, A E Roy) (Dordrecht: Kluwer Acad. Publ., 1999) p. 385
94. Kuranov A G, Postnov K A, Prokhorov M E *Astron. Zh.* **78** 717 (2001) [*Astron. Rep.* **45** 620 (2001)]
95. Kiel P D, Hurley J R *Mon. Not. R. Astron. Soc.* **369** 1152 (2006)
96. Yungelson L R et al. *Astron. Astrophys.* **454** 559 (2006)
97. Colbert E J M, Ptak A F *Astrophys. J. Suppl.* **143** 25 (2002)
98. Mushotzky R *Prog. Theor. Phys. Suppl.* **155** 27 (2004); astro-ph/0411040
99. Fabbiano G *Annu. Rev. Astron. Astrophys.* **27** 87 (1989)
100. Colbert E J M, Mushotzky R F *Astrophys. J.* **519** 89 (1999)
101. Miller M C, Colbert E J M *Int. J. Mod. Phys. D* **13** 1 (2004)
102. King A R et al. *Astrophys. J.* **552** L109 (2001)
103. Postnov K A *Pis'ma Astron. Zh.* **29** 372 (2003) [*Astron. Lett.* **29** 424 (2003)]
104. Soria R, Cropper M, Motch C *Chinese J. Astron. Astrophys. Suppl.* **5** 153 (2005); astro-ph/0409130
105. Podsiadlowski Ph, Rappaport S, Han Z *Mon. Not. R. Astron. Soc.* **341** 385 (2003)
106. Grishchuk L P et al. *Usp. Fiz. Nauk* **171** 3 (2001) [*Phys. Usp.* **44** 1 (2001)]
107. Nelemans G, in *The Astrophysics of Gravitational Wave Sources* (AIP Conf. Proc., Vol. 686, Ed. J M Centrella) (Melville, NY: AIP, 2003) p. 263
108. Cooray À *Mon. Not. R. Astron. Soc.* **354** 25 (2004)
109. Abbott B et al. (LIGO Sci. Collab.) *Class. Quantum Grav.* **23** S29 (2006); *Phys. Rev. Lett.* **94** 181103 (2005); *Phys. Rev. D* **69** 082004 (2004); *Nucl. Instrum. Meth. Phys. Res. A* **517** 154 (2004)
110. Chandrasekhar S *Phys. Rev. Lett.* **24** 611 (1970)
111. Friedman J L, Schutz B F *Astrophys. J.* **222** 281 (1978)
112. Kokkotas K D, Stergioulas N *Astron. Astrophys.* **341** 110 (1999)
113. Andersson N, Kokkotas K D, Stergioulas N *Astrophys. J.* **516** 307 (1999)
114. Shapiro S L, Teukolsky S A *Black Holes, White Dwarfs, and Neutron Stars* (New York: Wiley-Interscience, 1983) [Translated into Russian: Pt. 2 (Moscow: Mir, 1985) p. 505]
115. Mironovskii V N *Astron. Zh.* **42** 977 (1965) [*Sov. Astron.* **9** 752 (1966)]
116. Lipunov V M, Postnov K A, Prokhorov M E *Astron. Astrophys.* **176** L1 (1987)
117. LIGO Hanford Observatory, http://www.ligo-wa.caltech.edu/
118. Phinney E S *Astrophys. J.* **380** L17 (1991)
119. van den Heuvel E P J, Lorimer D R *Mon. Not. R. Astron. Soc.* **283** L37 (1996)
120. Burgay M et al. *Nature* **426** 531 (2003)
121. Kalogera V et al. *Astrophys. J.* **601** L179 (2004)
122. Lipunov V M *Grav. Cosmol.* **11** 166 (2005); astro-ph/0406502
123. Tutukov A V, Yungel'son L R *Mon. Not. R. Astron. Soc.* **260** 675 (1993)
124. Lipunov V M, Postnov K A, Prokhorov M E *New Astron.* **2** 43 (1997)
125. Lipunov V M, Postnov K A, Prokhorov M E *Astron. Astrophys.* **310** 489 (1996)
126. Willems B et al. *Astrophys. J.* **625** 324 (2005)
127. Hut P, Bahcall J N *Astrophys. J.* **268** 319 (1983)
128. Heggie D C, Hut P *Astrophys. J. Suppl.* **85** 347 (1993)
129. Rasio F A, McMillan S, Hut P *Astrophys. J.* **438** L33 (1995)
130. Fregeau J M et al. *Mon. Not. R. Astron. Soc.* **352** 1 (2004)
131. Hills J G *Astron. J.* **102** 704 (1991)
132. Aarseth S J *Gravitational N-Body Simulations* (Cambridge: Cambridge Univ. Press, 2003)
133. Gualandris A, Portegies Zwart S, Eggleton P P *Mon. Not. R. Astron. Soc.* **350** 615 (2004)

134. Popov S B, Prokhorov M E *Tr. Gos. Astron. Inst. im. Sternberga Ser. Nauchnaya* **72** 1 (2003)
135. Baym G, Lamb F K, in *Encyclopedia of Physics* 3rd ed. (Eds R G Lerner, G L Trigg) (Weinheim: Wiley-VCH, 2005) p. 1721; physics/0503245
136. Arzoumanian Z, Chernoff D F, Cordes J M *Astrophys. J.* **568** 289 (2002)
137. Hobbs G et al. *Mon. Not. R. Astron. Soc.* **360** 974 (2005)
138. Faucher-Giguère C-A, Kaspi V M *Astrophys. J.* **643** 332 (2006)
139. Zhang W, Woosley S E, Heger A, astro-ph/0701083
140. Eliseeva S A, Popov S B, Beskin V S, astro-ph/0611320
141. Beskin V S, Gurevich A V, Istomin Ya N *Physics of the Pulsar Magnetosphere* (Cambridge: Cambridge Univ. Press, 1993)
142. Ginzburg V L *Dokl. Akad. Nauk SSSR* **156** 43 (1964) [*Sov. Phys. Dokl.* **9** 329 (1964)]
143. Thompson C, Duncan R C *Astrophys. J.* **408** 194 (1993)
144. Beskin V S *Usp. Fiz. Nauk* **169** 1169 (1999) [*Phys. Usp.* **42** 1071 (1999)]
145. Contopoulos I, Spitkovsky A *Astrophys. J.* **643** 1139 (2006)
146. Pacini F *Nature* **216** 567 (1967)
147. Ruderman M, astro-ph/0510623
148. Yakovlev D G, Levenfish K P, Shibanov Yu A *Usp. Fiz. Nauk* **169** 825 (1999) [*Phys. Usp.* **42** 737 (1999)]
149. Regimbau T, de Freitas Pacheco J A *Astron. Astrophys.* **374** 182 (2001)
150. Page D, Geppert U, Weber F *Nucl. Phys. A* **777** 497 (2006)
151. Vranesevic N et al. *Astrophys. J.* **617** L139 (2004)
152. Konenkov D Yu, Popov S B *Pis'ma Astron. Zh.* **23** 569 (1997) [*Astron. Lett.* **23** 498 (1997)]
153. Lyne A G, Lorimer D R *Nature* **369** 127 (1994)
154. Beskin V S, Eliseeva S A *Pis'ma Astron. Zh.* **31** 648 (2005) [*Astron. Lett.* **31** 579 (2005)]
155. Taylor J H, Manchester R N, Lyne A G *Astrophys. J. Suppl.* **88** 529 (1993)
156. Bombaci I, Popov S B *Astron. Astrophys.* **424** 627 (2004)
157. Gonthier P L, Van Guilder R, Harding A K *Astrophys. J.* **604** 775 (2004)
158. Crawford F et al. *Astrophys. J.* **652** 1499 (2006)
159. Beskin V S, Eliseeva S A *Pis'ma Astron. Zh.* **31** 290 (2005) [*Astron. Lett.* **31** 263 (2005)]
160. Palomba C *Mon. Not. R. Astron. Soc.* **359** 1150 (2005)
161. Regimbau T, de Freitas Pacheco J A *Astron. Astrophys.* **447** 1 (2006)
162. Stella L et al. *Astrophys. J.* **634** L165 (2005)
163. Popov S B, Stern B E *Mon. Not. R. Astron. Soc.* **365** 885 (2006)
164. Blaes O, Rajagopal M *Astrophys. J.* **381** 210 (1991)
165. Manning R A, Jeffries R D, Willmore A P *Mon. Not. R. Astron. Soc.* **278** 577 (1996)
166. Brisken W F et al. *Astron. J.* **126** 3090 (2003)
167. Ikhsanov N R *Astron. Astrophys.* **399** 1147 (2003)
168. Popov S B et al. *Astrophys. J.* **530** 896 (2000)
169. Lipunov V M, Popov S B *Astron. Zh.* **72** 711 (1995) [*Astron. Rep.* **39** 632 (1995)]
170. Lipunov V M *Astrofizika Neitronnykh Zvezd* (Astrophysics of Neutron Stars) (Moscow: Nauka, 1987) [Translated into English (Berlin: Springer-Verlag, 1992)]
171. Popov S B et al. *Astrophys. J.* **544** L53 (2000)
172. Popov S B et al. *Astron. Astrophys.* **406** 111 (2003)
173. Popov S B et al. *Astrophys. Space Sci.* **299** 117 (2005)
174. Prokhorov M E, Popov S B, in *Fizika Kosmosa: Trudy 31-i Mezhdunar. Studencheskoi Nauchnoi Konf., Ekaterinburg, 2002* (Physics of Cosmos: Proc. 31st Intern. Student Sci. Conf., Ekaterinburg, 2002) (Ed. P E Zakharova) (Ekaterinburg: Izd. Ural'skogo Gos. Univ., 2002) p. 80
175. Popov S et al. *Astron. Astrophys.* **448** 327 (2006)
176. Popov S B, Grigorian H, Blaschke D *Phys. Rev. C* **74** 025803 (2006)
177. Popov S B et al., in *Quarks-2006* (Eds V Rubakov et al.) (2007) (in press)
178. Posselt B, Popov S B et al. (in preparation)
179. Popov S B, Treves A, Turolla R, in *4th AGILE Workshop* (Eds M Tavani, A Pellizzoni, S Vercellone) (Roma: Aracne Editrice, 2004) p. 183
180. Tolstoy E, in *The Scientific Requirements for Extremely Large Telescopes: Proc. of the 232nd IAU Symp.* (Eds P A Whitelock, M Dennefeld, B Leidundgeit) (Cambridge: Cambridge Univ. Press, 2006) p. 293; astro-ph/0604065
181. Zhang F et al. *Mon. Not. R. Astron. Soc.* **350** 710 (2004)
182. Marigo P, astroph/0701536
183. Leitherer C, in *The Evolution of Starbursts* (AIP Conf. Proc., Vol. 783, Eds S Hüttemeister et al.) (Melville, NY: AIP, 2005) p. 280; astro-ph/0409407
184. Bruzual G, astro-ph/0701907
185. Maeder A, Meynet G *Astron. Astrophys.* **361** 159 (2000)
186. Meynet G, Maeder A *Astron. Astrophys.* **429** 581 (2005)
187. Vazquez G A et al. *Astrophys. J.* (in press); astro-ph/0703699
188. Mas-Hesse J M, Cerviño M, in *Wolf–Rayet Phenomena in Massive Stars and Starburst Galaxies: Proc. of the 193rd IAU Symp.* (Eds K A van der Hucht, G Koenigsberger, P R J Eenens) (San Francisco, Calif.: Astron. Soc. of the Pacific, 1999) p. 550; Zhang F et al. *Astron. Astrophys.* **415** 117 (2004)
189. Zhang F et al. *Mon. Not. R. Astron. Soc.* **357** 1088 (2005)
190. Zhang F, Li L, Han Z *Mon. Not. R. Astron. Soc.* **364** 503 (2005)
191. De Donder E, Vanbeveren D *New Astron. Rev.* **48** 861 (2004)
192. Negueruela I, in *Active OB-Stars: Laboratories for Stellar and Circumstellar Physics* (ASP Conf. Ser., Vol. 361, Eds S Štefl, S P Owocki, A T Okazaki) (San Francisco, Calif.: Astron. Soc. of the Pacific, 2007); astro-ph/0601347
193. Leitherer C, in *The Spectral Energy Distributions of Gas-Rich Galaxies: Confronting Models with Data* (AIP Conf. Proc., Vol. 761, Eds C C Popescu, R J Tuffs) (Melville, NY: AIP, 2005) p. 39; astro-ph/0411345
194. Fritze-v.Alvensleben U, Bicker J *Astron. Astrophys.* **454** 67 (2006)
195. Bell E F, de Jong R S *Astrophys. J.* **550** 212 (2001)
196. Madau P, Ghisellini G, Fabian A C *Mon. Not. R. Astron. Soc.* **270** L17 (1994)
197. Pompilio F, La Franca F, Matt G *Astron. Astrophys.* **353** 440 (2000)
198. Antonucci R *Annu. Rev. Astron. Astrophys.* **31** 473 (1993)
199. Gilli R, Salvati M, Hasinger G *Astron. Astrophys.* **366** 407 (2001)
200. Gandhi P, Fabian A C *Mon. Not. R. Astron. Soc.* **339** 1095 (2003)
201. Halevin A V, astro-ph/0309176
202. Ueda Y et al. *Astrophys. J.* **598** 886 (2003)
203. Franceschini A, Braito V, Fadda D *Mon. Not. R. Astron. Soc.* **335** L51 (2002)
204. Ballantyne D R et al. *Astrophys. J.* **653** 1070 (2006)